

Thermodynamic Properties and Phase Transitions in a Mean-Field Ising Spin Glass on Lattice Gas: the Random Blume-Emery-Griffiths-Capell Model

Andrea Crisanti and Luca Leuzzi
 Department of Physics and SMC INFN Center,
 University of Rome I, "La Sapienza",
 Piazzale A. Moro 2, 00185, Rome, Italy
 (Dated: April 14, 2024)

The study of the mean-field static solution of the Random Blume-Emery-Griffiths-Capell model, an Ising-spin lattice gas with quenched random magnetic interaction, is performed. The model exhibits a paramagnetic phase, described by a stable Replica Symmetric solution. When the temperature is decreased or the density increases, the system undergoes a phase transition to a Full Replica Symmetry Breaking spin-glass phase. The nature of the transition can be either of the second order (like in the Sherrington-Kirkpatrick model) or, at temperature below a given critical value, of the first order in the Ehrenfest sense, with a discontinuous jump of the order parameter and accompanied by a latent heat. In this last case coexistence of phases takes place. The thermodynamics is worked out in the Full Replica Symmetry Breaking scheme, and the relative Parisi equations are solved using a pseudo-spectral method down to zero temperature.

Since its discovery, the spin glass (SG) phase has played and still plays a fundamental role in the investigation and understanding of many basic properties of disordered and complex systems. The analysis of the mean-field approximation of theoretical models displaying such a phase has revealed different possible scenarios, including different kinds of transition from the paramagnetic phase to the SG phase, as well as different kinds of SG phases. Most of the work, however, has been concentrated on just two scenarios.

In order of appearance in literature the first scenario is described by a Full Replica Symmetry Breaking (FRSB) solution characterized by a continuous order parameter function,¹ which continuously grows from zero by crossing the transition. The prototype model is the Sherrington-Kirkpatrick (SK) model,² a fully connected Ising-spin model with quenched random magnetic interactions.

The second scenario, initially introduced by Derrida by means of the Random Energy Model (REM),³ provides a transition with a jump in the order parameter to a stable low temperature phase in which the replica symmetry is spontaneously broken only once. The order parameter is a step function taking two values q_{min} and the so-called Edwards-Anderson order parameter,⁴ q_{EA} , (else said self-overlap), with $q_{\text{min}} < q_{\text{EA}}$. In the paramagnetic phase they are both equal to zero. At the transition, q_{EA} grows to a value larger than q_{min} . No discontinuity appear, however, in the thermodynamic functions. Actually, at the transition to the one step Replica Symmetry Breaking (1RSB) SG phase, the Edwards-Anderson order parameter q_{EA} can either grow continuously from zero or jump discontinuously to a finite value. The

first case of this second scenario includes Potts-glasses with three or four states,⁵ the spherical p -spin spin-glass model in strong magnetic field⁶ and some inhomogeneous spherical p -spin model with a mixture of $p = 2$ and $p > 3$ interactions.^{7,8} The latter case includes, instead, Potts-glasses with more than four states⁵, quadrupolar

glass models,^{5,9} p -spin interaction spin-glass models with $p > 2$,^{10,11,12} and the spherical p -spin spin-glass model in weak magnetic field.⁶ Because of the discontinuity of the overlap parameter across the transition the models belonging to this second case, often referred to as "discontinuous spin glasses" (see, for instance, Ref. [13]), have been widely investigated in the last years because of their relevance for the structural glass transition.^{11,14}

In all scenarios discussed above no latent heat occurs, i.e. the phase transition is continuous in the Ehrenfest sense. In this paper, instead, we consider a spin glass model undergoing (below a given critical point) a true thermodynamic first order phase transition between a paramagnetic (PM) and a Full Replica Symmetry Breaking (FRSB) SG phase, presenting coexistence of phases and latent heat, completing the work presented in Ref. [15].

Such a model is a generalization of the Blume-Emery-Griffiths-Capell (BEGC) model^{16,17} for the transition and the phase separation in the mixtures of He^3 - He^4 in a crystal field, in which a quenched disordered magnetic interaction is introduced. In that case the phase diagram consisted of a fluid phase, a superfluid one and a mixed phase (see Fig. 1 for a pictorial representation of the diagram).

The first study of a spin-glass model undergoing a genuine first order thermodynamic transition is the Gatak-Sherrington model (GS),¹⁸ a simplified version of the model under current investigation. In this spin-1 model in crystal field, no biquadratic coupling is considered: the Replica Symmetric (RS) solution and its stability have been carried out by Lage and Almeida,¹⁹ Motishaw and Sherrington²⁰ and da Costa et al.²¹, albeit not always with compatible results. There the evidence for a first order phase transition was found, in the neighborhood of the tricritical point.

In the last few years some work has been devoted to the comprehension of the Random generalization of the BEGC model (RBEGC), mostly at the level of the RS

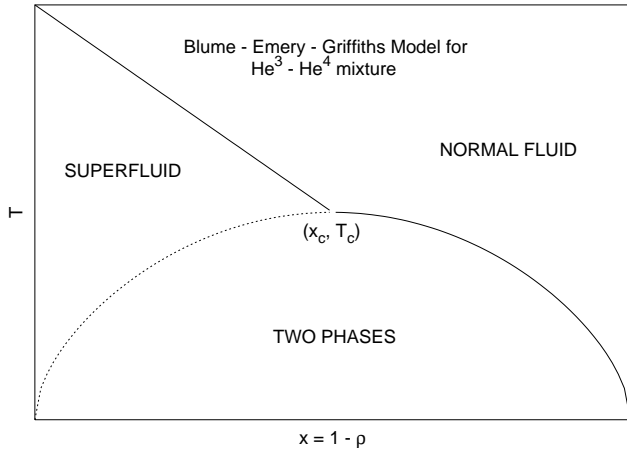


FIG. 1: The phase diagram of the mean-field model for He^3 - He^4 mixture as originally studied by BEG. x is the density of He^3 particles and p the density of He^4 .

solution, that turns out to be unstable as soon as the transition takes place. Such an analysis has been performed in Refs. [22,23] for what concerns the lattice gas version of the model, and in Refs. [24,25,26,27] for the spin-1 model. For sake of completeness we also report the study [28] where, together with the random magnetic interaction, also a random biquadratic interaction is considered.

Quite recently, the spherical version of the present model has been worked out exhaustively for positive and null particle-particle interaction, both statically and dynamically, by Caiazzo et. al.^{29,30}.

In section I we present the model, also indicating the connection with different notation in the literature. In Sec. II the replica formalism for the model is recalled, the Replica Symmetric (RS) solution presented, together with its stability and low temperature analysis. In Sec. III we adapt the variational method for the FRSB solution⁴⁰ to the model, we explain the numerical method of resolution applied and we discuss the practical necessity of using different gauges to express the thermodynamic functional in different parameters regions. In Sec. IV we study the thermodynamic observables. From the behavior of the entropy versus temperature at fixed chemical potential we observe that below the tricritical point the transition involves latent heat. In Sec. V we display the phase diagrams in the parameters T , x and density. Sec. VI contains our conclusions.

I. THE RANDOM

BLUME-EMERY-GRIFFITHS-CAPEL MODEL

There exist two completely equivalent versions of this disordered model (at least as far as the statics is concerned). One version is a direct generalization of the

BEGC model, with spin 1 variables ($S_i = 1; 0; -1$ on site i),²⁴ the other one is a lattice gas of Ising spins (spin $S_i = 1; -1$, with occupation numbers $n_i = 0; 1$ on site i).^{22,23}

In this paper we will use the second formulation described, in the mean-field approximation, by the Hamiltonian²³

$$H = \sum_{i < j} J_{ij} S_i S_j n_i n_j - \frac{K}{N} \sum_{i < j} n_i n_j - \sum_i h_i S_i n_i; \quad (1)$$

where the Ising spin glass lattice gas in an external magnetic field is coupled to a spin reservoir by the chemical potential μ . K is the particle-particle coupling constant and h the external magnetic field. The magnetic interaction is described by quenched Gaussian random variables J_{ij} , symmetric in $i \leftrightarrow j$, with mean $\overline{J_{ij}} = J_0 = N$ and variance $\overline{J_{ij}^2} = \overline{J_{ji}^2} = J^2 = N$. Here and in the following the overline denotes average with respect to disorder.

Just for completeness we also report the Hamiltonian in the original formulation:

$$H = \sum_{i < j} J_{ij} \sigma_i \sigma_j - \frac{K}{N} \sum_{i < j} (\sigma_i \sigma_j)^2 + D \sum_i \sigma_i^2 - \sum_i h_i \sigma_i; \quad (2)$$

The transformation $\sigma_i = S_i n_i$, between the spin lattice gas dynamic variables and the spin-1 variables σ_i , and the transformation $D = T \log 2$, between D and the crystal field D of the spin-1 system, allow for a perfect equivalence of two versions of the model.

Some limiting cases of the model are the SK model² (for $J = 1$) and the site frustrated percolation model³¹ (for $K = 1$ and $J = 1$).

In most cases studied up to now^{18,19,20,21,22,23,24,25,26,27} the analysis was mainly limited to the RS solution. The general picture which emerged was an instability of the RS solution below some transition line in the region of low temperature and large density of particles. The nature of the SG phase (1RSB of FRSB) and the type of transition (SK-like¹, p-spin-like¹⁰ or different²⁰) were, however, not clear, also due to some "anomalous" properties at the RS level such as, for instance, complex stability eigenvalues. Despite this fact, the possibility of a p-spin-like transition has put new interest into this model as a possible, more realistic, model for the structural glasses, and its finite dimensions version has been numerically investigated in a search for evidence of a structural glass transition scenario^{32,33}. Performing the quenched averages in the most general Replica scheme of computation it has been possible to show that the stable solution in the mean-field case, is FRSB everywhere in the SG phase, where spins are frozen.¹⁵

II. THE REPLICA TRICK FOR THE THERMODYNAMICS OF DISORDERED SYSTEMS

For any fixed (quenched) coupling realization J , the partition function of a system of N dynamic (annealed) variables, is given by^{34,35}

$$Z_N[J] = \text{Tr} \exp H[J; \sigma] \quad (3)$$

and the quenched free energy per spin is

$$f_N = \frac{1}{N} \overline{\log Z_N} = \frac{1}{N} \sum_{J \in \mathcal{J}} d[J] P[J] \log Z_N[J] \quad (4)$$

where $(\overline{})$ indicates the average over the couplings realizations. The thermodynamic limit of the free energy,

$\lim_{N \rightarrow \infty} \frac{1}{N} \log Z_N[J] = N$ is well defined and equal to the quenched free energy $f = \lim_{N \rightarrow \infty} \frac{1}{N} f_N$ for almost any coupling realization J (self-average property).

The analytic computation of the quenched free energy, i.e., of the average of the logarithm of the partition function, is quite a difficult problem, even in simple cases as nearest neighbor one dimensional models. However, since the integer moments of the partition function are easier to compute, the standard method involves the so called "replica trick" by considering the annealed free energy $f(n)$ of n non-interacting 'replicas' of the system,^{2,34,35}

$$f(n) = \lim_{N \rightarrow \infty} \frac{1}{N} \log \overline{(Z_N[J])^n} \quad (5)$$

The quenched free energy of the original system is then recovered as the continuation of $f(n)$ down to the unphysical limit $n = 0$,⁵⁴

$$f = \lim_{n \rightarrow 0} \lim_{N \rightarrow \infty} \frac{\overline{(Z_N[J])^n}}{N} = \lim_{n \rightarrow 0} f(n) \quad (6)$$

In the last equality we assumed that the replica limit and the thermodynamic limit can be exchanged. This procedure replaces the original interactions in the real space with couplings among different replicas. The interested reader can find a complete and detailed presentation of the replica method for disordered statistical mechanical systems in Refs. [34] and [35].

Applying the replica trick to the computation of the thermodynamic potential of the random BEG-C model we find, in the saddle point approximation for large N ,

$$\overline{Z_N[J]^n} = \exp f(n) \quad (7)$$

$$f = \frac{K}{2} \frac{1}{n} \sum_{a=1}^n \sum_{b=1}^n J_{ab}^2 + \frac{J_0}{2} \frac{1}{n} \sum_{a=1}^n m_a^2 + \frac{(J)^2}{4} \frac{1}{n} \sum_{a \neq b} q_{ab}^2 - \frac{1}{n} \log Z^0 \quad (8)$$

$$Z^0 = \int \prod_{a=1}^n \int \prod_{b=1}^n \exp f[H^0[f dg; fm g; f q g]] \quad (9)$$

$$H^0[f dg; fm g; f q g] = \sum_{a=1}^n \sum_{b=1}^n S_a n_a (J_0 m_a + h) + \frac{(J)^2}{2} \sum_{a \neq b} q_{ab} S_a n_a S_b n_b \quad (10)$$

where the sum in the one-site partition Z^0 is taken over all the possible values of the spins S_a and the occupation numbers n_a . Here and everywhere else in this paper we use the abbreviation

$$K = K + \frac{J^2}{2} \quad (11)$$

The saddle point equations, coming from the extremization of Eq. (8), give the self-consistent relations

$$q_{ab} = h S_a n_a S_b n_b \quad (12)$$

$$n_a = \overline{n_a} \quad (13)$$

$$m_a = h S_a n_a \quad (14)$$

where $\overline{}$ is the average computed over the measure $\exp(-H^0)$.

The parameter n_a represents the density of the replica a . In the thermodynamic limit this is equal to $\frac{1}{n} \sum_i n_i = \overline{n_i}$ which, in the Hamiltonian (1), is only coupled to the chemical potential, that is a replica independent quantity. The density is therefore equal for each replica: $n_a = \frac{1}{n}$; $\forall a = 1, \dots, n$.

The same holds for m_a which is coupled to the external field h : $m_a = m$; $\forall a = 1, \dots, n$. It generally holds that one index quantities are replica invariant.³⁴

A. Replica Symmetric Solution and Stability of the Paramagnetic Phase

The replica symmetric free energy is obtained by evaluating Eq. (8) at $q_{ab} = q_0$, for $a \neq b$, $n_a = \frac{1}{n}$ and $m_a = m$ for every a ; b and it reads²³

$$f = \frac{K}{2} + \frac{J_0}{2} m^2 - \frac{(J)^2}{4} q_0^2 - \int_0^1 dy P_0(y) \phi_0(y) \quad (15)$$

with

$$\phi_0 = \frac{(J)^2}{2} (q_0 + K) + \quad (16)$$

$$P_0(y) = \frac{1}{2} \exp \frac{(y - m J_0 - J h)^2}{2 q_0} \quad (17)$$

$$\phi_0(y) = \frac{1}{J} \log [2 + 2 e^{-\phi_0} \cosh J y] \quad (18)$$

The order parameters q_0 and m satisfy the following self-consistency equations (see App. VI for the details of

derivation):

$$\rho = \frac{1}{Z_1} \int dy P_0(y) \sim (y) \quad (19)$$

$$q_0 = \frac{1}{Z_1} \int dy P_0(y) m^2(y) \quad (20)$$

$$m = \frac{1}{Z_1} \int dy P_0(y) m(y) \quad (21)$$

with the following definitions

$$\sim(y) = \frac{\cosh Jy}{e^0 + \cosh Jy} \quad (22)$$

$$m(y) = \frac{\sinh Jy}{e^0 + \cosh Jy} \quad (23)$$

The eigenvalues of the Hessian of Eq. (8) computed in the RS approximation are derived in appendix VI, where the stability analysis is carried out.

In the case $J_0 = h = 0$ only the paramagnetic solution ($q_0 = 0$) is stable, so that Eqs. (19)-(21) reduce to

$$q_0 = 0; \quad \rho = \frac{1}{1 + e^{-K}}; \quad m = 0; \quad (24)$$

and the eigenvalues of independent modes are

$$\lambda_0 = (J)^2 \frac{1}{h} - (J)^2 \frac{1}{K} \quad (25)$$

$$\lambda_1 = K \frac{1}{j} - K \frac{1}{K} \quad (26)$$

where λ_0 is connected to q - q fluctuations, whereas λ_1 is the stability eigenvalue of the density-density fluctuations. In the above formulas we have considered both the case in which $K > 0$ and $K < 0$. The last one occurring only if the particle-particle interaction K is negative and when T is bigger than $1/(2K)$.

The lines $\lambda_0 = 0$ and $\lambda_1 = 0$ delimit the stability region for the RS solution on the phase diagram. In the T - ρ phase diagram the stable region is for

$$T > J \quad (27)$$

$$T > \frac{K}{2} \left(1 + \frac{1}{K} \right) + \frac{J^2}{K^2} \frac{2}{(1 + \frac{1}{K})} \quad (28)$$

corresponding, respectively, to $\lambda_0 > 0$ and $\lambda_1 > 0$.

For any value of K , there is one intersection between $\lambda_0 = 0$ and $\lambda_1 = 0$, namely the tricritical point:

$$\frac{T_c}{J} = \frac{J}{2K} - \frac{3}{2} + \frac{K}{J} + \frac{K^2}{J^2} \frac{K}{J} + \frac{9}{4} \quad (29)$$

$$\frac{c}{J} = \frac{1}{2} - \frac{K}{J} + \log \frac{1}{c} - 1; \quad (30)$$

where c is obtained from the paramagnetic expression (19-22) for ρ . In table I we list some values of interest of the tricritical values and in Fig. 2 we plot their behavior as function of the particle-particle coupling constant.

$K = J$	1	1	0	-1	1
$T_c = J \frac{c}{J}$	1	1/2	1/3	0.21922	0
$c = J$	1	-1	-0.73105	-0.55923	0

TABLE I: Critical values of the thermodynamic parameters for some specific particle-particle interaction values. Parameters are expressed in units of J .

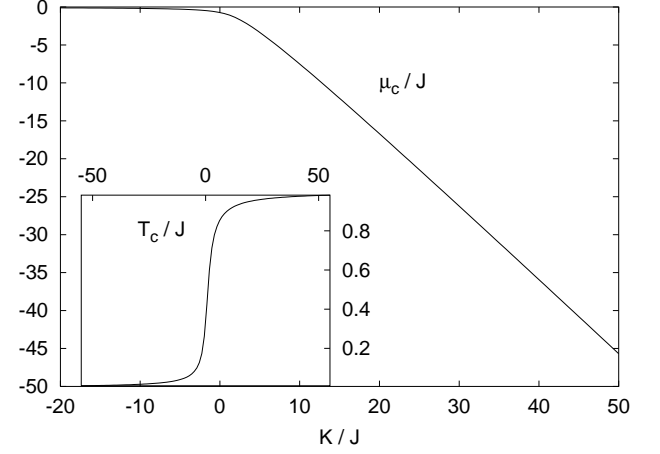


FIG. 2: The values of the thermodynamic parameters (in units of J) at the tricritical point as a function of the particle-particle coupling constant. The critical density is equal to T_c .

As K decreases, the critical temperature goes to zero. As we will see in the following, in Sec. V where we study the phase diagrams, this implies that the phase diagram region of phase coexistence progressively reduces itself. The critical value of the chemical potential grows to zero as K tends to -1 : in order to contrast large particle repulsion a larger chemical potential (in the limit non-negative) is needed.

1. Thermodynamic Observables in the Replica Symmetric Solution

The internal energy and the entropy take the form:

$$u = \frac{K}{2} + \frac{J^2}{2} \rho^2 - J_0 m^2 - h m + \frac{J^2}{4} q_0^2 \quad (31)$$

$$s = -\frac{(J)^2}{4Z_1} \left(\frac{q}{J} \right)^2 - \rho \int dy P_0(y) [\rho_0(y) - y m(y)] \quad (32)$$

Integrating by part we can derive:

$$\frac{1}{Z_1} \int dy P_0(y) y m(y) = J \left(\frac{q}{J} \right) \quad (33)$$

The entropy, then, becomes

$$s = \frac{(J)^2}{4} \left(\frac{q}{Z} \right)^2 + \int_0^1 dy P_0(y) \ln P_0(y) \quad (34)$$

B. Low Temperature Behavior of the RS Solution

It can be of some help for later purposes and also to make a comparison with existing results, to probe how the observables behave in the very low temperature limit, even in this case for which the SG solution is unstable. We simplify the discussion to the case $J_0 = h = 0$. Putting $z = y = \frac{p}{q}$ as integration variable in the above expressions the entropy can be written as

$$s = \frac{(J)^2}{4} \left(\frac{q}{Z} \right)^2 + \int_0^1 \frac{dz}{2} e^{-z^2/2} \left[\ln f_0(z) - \frac{p}{q} z \ln(z) \right] \quad (35)$$

We define

$$a = \frac{0}{J} \quad (36)$$

$$C = \frac{J}{Z} \left(\frac{q}{Z} \right) \quad (37)$$

$$I = \int_0^1 \frac{dz}{2} e^{-z^2/2} f_0(z) - \frac{p}{q} z \ln(z) g \quad (38)$$

We consider two cases separately in the zero temperature limit.

1. Full system : $a = 0$

$$\lim_{J \rightarrow 1} \bar{m} = 1 \quad (39)$$

$$\lim_{J \rightarrow 1} C = \frac{r}{2} \quad (40)$$

$$\lim_{J \rightarrow 1} a = \frac{1}{2} + \frac{K}{J} \quad (41)$$

$$I = 0 + O(\Gamma) \quad (42)$$

$$s = \frac{1}{2} + O(\Gamma) \quad (43)$$

2. Partially diluted system : $a < 0$

$$\lim_{J \rightarrow 1} \bar{m} = \bar{m} < 1 \quad (44)$$

$$\lim_{J \rightarrow 1} C = \bar{C} \quad (45)$$

$$\lim_{J \rightarrow 1} a = \bar{a} = \frac{\bar{C}}{2} + \frac{K \bar{m}}{J} \quad (46)$$

with \bar{m} and \bar{C} given by the zero temperature self-consistency equations:

$$\bar{m} = \text{erfc} \frac{\bar{a}}{2} \quad (47)$$

$$\bar{C} = \frac{r}{2} \exp \frac{\bar{a}}{2} \quad (48)$$

Notice that as $a \rightarrow 0$ one obtains from the above equations: $\bar{m} = 1$ and $\bar{C} = \frac{r}{2}$.

Finally one gets

$$I = 0 + (1 - \bar{m}) \log 2 - \bar{C} \bar{a} \log 2 + O(\Gamma) \quad (49)$$

$$s = \frac{\bar{C}^2}{4} + (1 - \bar{m}) \log 2 - \bar{C} \bar{a} \log 2 + O(\Gamma) \quad (50)$$

For fixed K and J there is, thus, a limiting (negative) value of the chemical potential below which the lattice will not be full at zero temperature. For

$$\frac{r}{J} < \frac{1}{2} - \frac{K}{J} \quad (51)$$

the density (and the overlap) is equal to $\bar{m} < 1$.

In any case the asymptotic value of C is finite, yielding

$$q = T : \quad (52)$$

III. A VARIATIONAL METHOD FOR THE FULL REPLICAS SYMMETRY BREAKING SOLUTION IN DISORDERED SYSTEMS

To clarify which kind of transition takes place we improve the study of the static properties of the SG phase of the mean-field RBEGC, making use of the FRSB Parisi Ansatz. The first thing to notice is that the stable SG phase is always of FRSB type. The transition between the PM phase and the SG phase can be either of the SK-type or, below a given T_c , discontinuous with a jump in the entropy and hence a latent heat. Moreover for a certain range of parameters, the two phases, PM and SG, coexist. For any parameter choice we find no evidence for a p-spin-like transition with discontinuous order parameter.

The aim is to evaluate the $n \rightarrow 0$ limit in Eq. (8) with the Ansatz that the structure of the matrix Q follows a FRSB scheme. In order to be as general as possible, we shall use the RSB scheme introduced for the SK model by de Dominicis, Gabay and Orland,^{36,37} which besides the Edwards-Anderson order parameter⁴ also involves the anomaly to the linear response function, otherwise called Sompolinsky's anomaly.³⁸ The more usual Parisi's RSB scheme is, if necessary, eventually recovered by a proper gauge fixing, once that the limit of infinite number of replica symmetry breakings has been taken [see below Eq. (73)].

By applying the RSB scheme in finite times and introducing the two functions $q(x)$ (overlap function) and

$\phi(x)$ (anomaly function), $0 \leq x \leq 1$, the free energy functional, Eq. (8), becomes:

$$f = \frac{K}{2} + \frac{J_0}{2} m^2 - \frac{(J)^2}{4} q(1)^2 - \frac{J}{2} \int_0^1 dx \phi(x) - \phi(x) - \frac{J}{2} \int_1^1 dy P_0(y) \phi(0;y); \quad (53)$$

where $P_0(y)$ is defined as

$$P_0(y) = \frac{1}{2} \frac{\exp\left(\frac{(y - (h + J_0 m) - J)^2}{2q(0)}\right)}{q(0)} \quad (54)$$

and $\phi(0;y)$ is the solution, evaluated at $x = 0$, of the Parisi-parabolic equation¹

$$-\phi(x;y) = \frac{q(x)}{2} \phi(x;y) + \frac{-\phi(x)}{2} \phi(x;y)^2; \quad (55)$$

with the boundary condition at $x = 1$

$$\phi(1;y) = \phi_1(y) - (J)^{-1} \log 2 + 2e^{-1} \cosh Jy; \quad (56)$$

and

$$\begin{aligned} \phi_1 &= \frac{(J)^2}{2} \left[\phi(1) + \left(\frac{1}{2} + K \right) \right] \\ &= K + \frac{(J)^2}{2} q(1); \end{aligned} \quad (57)$$

The overlap $q(x)$, the density of occupied sites and the anomaly $\phi(x)$ are the order parameters.⁵⁵ We have used the standard notation and denoted derivatives with respect to x by a dot and derivatives with respect to y by a prime. In this notation Sompolinsky's ϕ^0 in Ref. 38 becomes our T .

The Parisi equation (55) can be included into a free energy variational functional via the Lagrange multiplier $P(x;y)$ and the initial condition at $x = 1$, Eq. (56), via $P(1;y)$.⁴⁰ The free energy functional is then

$$\begin{aligned} f_v &= f - \frac{J}{2} \int_1^1 dy P(1;y) [\phi(1;y) - \phi_1(y)] \\ &\quad - \frac{J}{2} \int_1^1 dx \int_1^1 dy P(x;y) - \phi(x;y) \\ &\quad + \frac{q(x)}{2} \phi(x;y) - \frac{-\phi(x)}{2} \phi(x;y)^2; \end{aligned} \quad (58)$$

with $P_0(y)$ and $\phi_1(y)$ defined in Eqs. (54, 56).

By such a construction f_v is stationary with respect to variations of $P(x;y)$, $P(1;y)$, $\phi(x;y)$, $\phi(0;y)$, $q(x)$, $-\phi(x)$ and deriving with respect to ϕ . Variations of $P(x;y)$ and $P(1;y)$ simply give back Eqs. (55) and (56). Stationarity with respect to variations of $\phi(x;y)$ and $\phi(0;y)$ leads to a partial differential equation for $P(x;y)$:

$$P(x;y) = \frac{q(x)}{2} P(x;y) + \frac{-\phi(x)}{2} P(x;y) \phi(x;y)^0; \quad (59)$$

and to the boundary condition at $x = 0$

$$P(0;y) = P_0(y); \quad (60)$$

Eventually, variations of f_v with respect to $q(x)$, $-\phi(x)$ and the derivative with respect to ϕ lead to

$$\phi(x) = \frac{J}{2} \int_1^1 q(1) + dy P(x;y) \phi(x;y)^0; \quad (61)$$

$$q(x) = \frac{J}{2} \int_1^1 dy P(x;y) \phi(x;y)^2 \quad (62)$$

$$= \frac{J}{2} \int_1^1 dy P(1;y) \frac{\cosh Jy}{e^{-1} + \cosh Jy} \quad (63)$$

with $\phi(1) = 0$, the anomaly at the shortest time-scale, corresponding to $x = 1$, being zero by construction: the Fluctuation-Dissipation Theorem (FDT) holds at short time-scales.

The Lagrange multiplier $P(x;y)$ represents the distribution of local fields. One may indeed associate a given overlap $q(x)$ with a time scale x such that for times of order x states with an overlap equal to $q(x)$ or greater can be reached by the system (these time-scales completely decouple in the thermodynamic limit). In this picture the $P(x;y)$ becomes the probability distribution of frozen local fields y at the time scale labeled by x .⁴⁰

For the numerical treatment of the FRSB equations and also to allow for a clearer physical interpretation of the functions that we are analyzing, we define the local magnetization $m(x;y) = \phi(x;y)$, whose differential antiparabolic equation we derive from Eqs. (55), (56) as

$$m(x;y) = \frac{q}{2} m(x;y) + \frac{-\phi(x)}{2} m(x;y) m(x;y)^0; \quad (64)$$

$$m(1;y) = m_1(y) = \frac{\sinh(Jy)}{e^{-1} + \cosh(Jy)}; \quad (65)$$

The average equilibrium magnetization m can, then, be computed in terms of the local magnetization at $x = 0$:

$$m = \frac{\partial f}{\partial h} = \frac{J}{2} \int_1^1 dy P(0;y) m(0;y); \quad (66)$$

Another useful relation for the numerical evaluation of the order parameters and the thermodynamic functions built on them is got from the computation of the term $\int_0^1 dx \int_1^1 dy P(x;y) - \phi(x;y)$ in two different ways: once using Eq. (56) and, in the other case, applying Eq. (59) and integrating by part. From the comparison of the two results the following equation is obtained:

$$\begin{aligned} \int_1^1 dy P(1;y) \phi(1;y) &= \int_1^1 dy P(0;y) \phi(0;y) \\ &= \frac{1}{2} \int_0^1 dx q(x) - \phi(x) \end{aligned} \quad (67)$$

Deriving Eq. (61) with respect to x yields

$$\int_1^1 dy P(x;y) m(x;y)^0 = 1 \quad (68)$$

valid for every x and guaranteeing the marginal stability of the FRSB Ansatz.

The coupled equations (59), (64), with border conditions (60), (65) are the FRSB equations. In the following we are going to show how they can be numerically solved and what are the gauges we will use in order to get the most general SG phase and the order parameters characterizing the transition to it.

Differentiating once more Eq. (68) one finds

$$\frac{-}{q} = \frac{R_1}{R_1} \frac{1}{1} \frac{dy}{dy} P(x;y) m^0(x;y)^3 \quad (69)$$

that will become useful is the following when we will discuss the choice of the gauge to perform the numerical computation (see Sec. IIIB).

A. Numerical Integration of the FRSB Equations: the Pseudo-Spectral method

In order to study the low temperature regime of the RBEGC in the limit of a large number of clauses we have numerically integrated the FRSB equations (59)–(64) to determine $q(x)$, $P(x;y)$ and $m(x;y)$. We followed the iterative scheme of Refs. [40,41], but with an improved numerical method which allows for very accurate results for all temperatures (see Refs. [42,43]).

We start from an initial guess for $q(x)$, (x) and then $m(x;y)$, $P(x;y)$ and the associated $q(x)$ are computed in the order as:

1. Compute $m(x;y)$ integrating from $x = 1$ to $x = 0$ Eqs. (64) with initial condition (65).
2. Compute $P(x;y)$ integrating from $x = 0$ to $x = 1$ Eqs. (59) with initial condition (60).
3. Compute $q(x)$, (x) and using Eqs. (62–63).

The steps 1 ! 2 ! 3 are repeated until a reasonable convergence is reached, typically we require a mean square error on q , P and m of the order $O(10^{-6})$ and we checked that the identities (67), (81) and $1 - T = \bar{q}$ were satisfied to this precision as well. The number of iterations necessary are a few hundreds. The core of the integration scheme is the integration of the partial differential equations (59) and (64). In previous works this was carried out through direct integration in the real space which requires a large grid mesh to obtain precise results. To overcome this problem we move to the Fourier space where we can apply a pseudo-spectral⁴⁴ method of integration.

Indicating by $FT[o](x;k)$ the Fourier transform of function $o(x;y)$,

$$FT[o](x;k) = \frac{1}{N_y} \sum_{N_y=2}^Z dy e^{iky} o(x;y); \quad (70)$$

the FRSB Eq. (56), written in terms of the wave number k , becomes

$$m(x;k) = k^2 \frac{q(x)}{2} m(x;k) + ik \frac{-(x)}{2} FT[m^2](x;k) \quad (71)$$

and the FRSB Eq. (59) takes the form

$$P(x;k) = k^2 \frac{q(x)}{2} P(x;k) + ik \frac{-(x)}{2} FT[Pm](x;k) \quad (72)$$

For each value of k these are ordinary differential equations which can be integrated using standard methods. To avoid the time consuming calculation of the convolution in the nonlinear terms we use the pseudo-spectral code on a grid mesh of $N_x \times N_y$ points, covering the x interval $[0;1]$ and the y interval $[y_{max}; y_{max}]$. The truncation of the wave number may bring to anisotropic effects for large k . De-aliasing is, thus, performed by a $N_y=2$ truncation, which ensures a better isotropy of the numerical treatment. Eventually, the x integration is carried out by means of a third order Adams-Bashford scheme which reduces the number of fast Fourier transforms (FFT) calls.⁴⁵

Typical values used are $N_x = 500 \text{ } 1000$, $N_y = 1024 \text{ } 4096$ and $y_{max} = 24 \text{ } 48$. The difference between the values for N_x and the values for N_y comes from the fact that, if the solution in y is smooth enough, only a few low wave numbers k are excited. The value of the parameter y_{max} fixes the y range where the solution is assumed different from zero. Indeed, in the numerical algorithm is assumed that $P(x;y) = m(x;y) = 0$ for $|y| > y_{max}$. This explains the rather large value of y_{max} used.

B. Choice of Gauge

The solution to the spin-glass mean-field models obtained using the scheme of Sommers is overconstrained and the functional expression of $-(x)$ can be, thus, chosen in different ways, selecting, in this way, a gauge for the order parameters. The usually studied gauges are

$$-(x) = \int x q(x) \quad \text{Paris gauge}^1 \quad (73)$$

$$-(x) = (0) \quad \text{Sommers gauge}^{40} \quad (74)$$

where the anomaly is given by the stationarity Eq. (61) at $x = 0$. We rewrite it here in terms of the local magnetization

$$(0) = \int [q(1)] + \sum_{1}^Z dy P(0;y) m^0(0;y) \quad (75)$$

The anomaly at the largest time-scale is gauge invariant since it depends on the Edwards-Anderson parameter and on the derivative of the equilibrium local magnetization. $-(x)$ measures the violation of the linear response on the time-scale labeled by x . As such, it's a decreasing function of x , being zero at the shortest time-scale

nds

$$u = \frac{K + J^2}{2} \langle \sigma^2 \rangle + \frac{J_0}{2} m^2 \quad (80)$$

$$+ \frac{J^2}{2} \langle \sigma^2 \rangle - \frac{J^2}{2} \langle \sigma^2 \rangle^2 - \frac{J}{Z} \int_0^1 dx \langle \sigma(x) \rangle - \langle \sigma \rangle$$

$$+ \frac{J}{Z} \int_0^1 dy P(\sigma(y)) \ln P(\sigma(y))$$

The comparison between Eq. (79) and Eq. (80) yields the relation

$$\frac{1}{Z} \int_0^1 dx \langle \sigma(x) \rangle - \langle \sigma \rangle = \frac{J}{Z} \langle \sigma^2 \rangle - \frac{J^2}{2} \langle \sigma^2 \rangle^2 \quad (81)$$

$$+ \frac{J_0}{J} m^2 + \frac{h}{J} m + \frac{J}{Z} \int_0^1 dy P(\sigma(y)) \ln P(\sigma(y))$$

Taking the limit $J \rightarrow 1$, with $K = J = 0$ and choosing the gauge $\sigma = J \times q(x)$ (corresponding to the Parisi scheme for RSb) we get the SK formulas².

4. Entropy density

The entropy density $s = -\langle \ln P \rangle$ can be expressed either as

$$s = -\frac{1}{Z} \int_0^1 \frac{(J^2)}{4} \langle \sigma^2 \rangle \quad (82)$$

$$+ \frac{J}{Z} \int_0^1 dy P(\sigma(y)) \ln P(\sigma(y))$$

or, exploiting Eq. (81), as

$$s = -\frac{(J^2)}{4} \langle \sigma^2 \rangle - \frac{1}{Z} \int_0^1 (J^2) \langle \sigma^2 \rangle \langle \sigma \rangle \quad (83)$$

$$+ \frac{J_0}{Z} m^2 + \frac{h}{J} m + \frac{2}{Z} \int_0^1 dx \langle \sigma(x) \rangle - \langle \sigma \rangle$$

$$+ \frac{J}{Z} \int_0^1 dy P(\sigma(y)) \ln P(\sigma(y))$$

5. Compressibility

The compressibility in terms of the density of occupied sites and its conjugated field, the chemical potential, can be expressed in the FRSB formulation as:

$$\chi = \frac{1}{Z} \frac{\partial \langle \sigma \rangle}{\partial h} = \frac{1}{Z} \int_0^1 dy P(\sigma(y)) \frac{\partial \langle \sigma(y) \rangle}{\partial h} \quad (84)$$

where we define

$$\langle \sigma(y) \rangle = \frac{\cosh(Jy)}{e^{-1} + \cosh(Jy)} \quad (85)$$

In Fig. IV 5 we show the compressibility behavior versus temperature of the system with particle-particle interaction constant $K = J$ for three values of the chemical

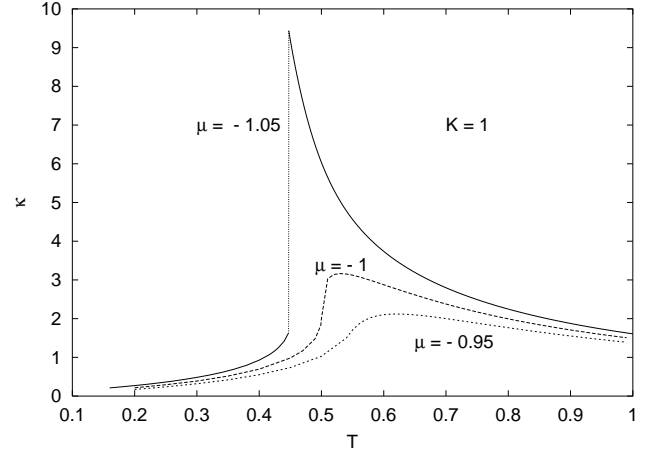


FIG. 3: Compressibility versus temperature for $K=J=1$, in units of J . The behavior at $T_c = J = 1$ is smooth at the transition (right dotted line). At T_c a discontinuity starts to develop (middle dashed curve) leading to a cusp for $T < T_c$ (left solid curve).

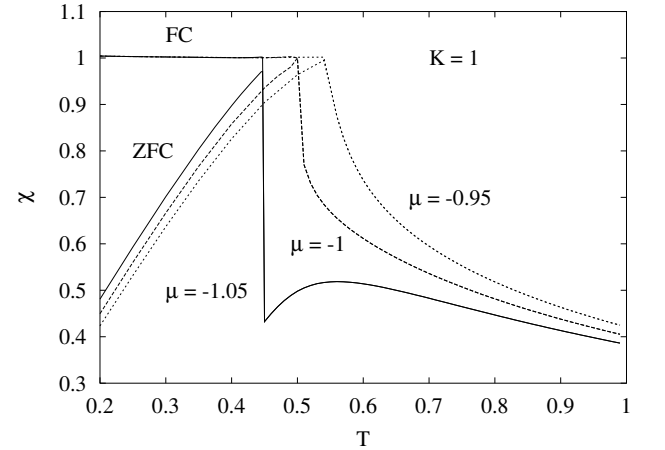


FIG. 4: Field cooled and zero-field cooled susceptibility for $K=1$. Above $T_c = 1$ FC (χ_0) and ZFC (χ_1) susceptibilities continuously reach the same value at the second order phase transition ($\chi_0 = \chi_1 = 1$ in absence of external magnetic field), whereas for $T < T_c$ both a discontinuity takes place and the value of χ_1 never reaches the one of χ_0 at the, now first order, phase transition.

potential. Respectively above, at and below the critical value T_c below which the transition happens to be first order in the Ehrenfest sense. For $T < T_c$ a cusp shows up and, decreasing the temperature, shrinks to a much lower value as the transition point is crossed.

6. Susceptibility

The magnetic susceptibility of the RBEGC model at equilibrium can be written either as

$$\chi_0 = J \int_0^1 dx q(x) \quad (86)$$

or, with the help of Eq. (66), as

$$\chi_0 = \frac{\partial m}{\partial h} = \int_1^{R_1} dy P(0;y) m^0(0;y); \quad (87)$$

whereas the susceptibility obtained when the system is constrained to stay in a single minimum of the free energy function comes out to be

$$\chi_1 = J [q(1)]: \quad (88)$$

The equilibrium susceptibility is a function of the average $\bar{q} = \int_0^1 dx q(x)$ of the overlap over all possible values it can take at all time scales ($0 \leq x \leq 1$). It corresponds to the Field-Cooled susceptibility. The second susceptibility, instead, only depends on the Edwards-Anderson parameter $q_{EA} = q(1)$. It physically expresses the self-overlap of configurations belonging to the same state. Indeed, at time scale 1, i.e., the shortest time scale, the system has not yet visited but one metastable state, thus the response to a field perturbation only depends on the self-overlap. The experimental analogue of χ_1 is the Zero Field Cooled susceptibility. As a matter of fact, also in that case the system remains in one single state during the cooling down to the SG phase, since it is not driven by any external field.

From a dynamical point of view, the equilibrium susceptibility χ_0 can otherwise be expressed in terms of the function $q(x)$ defined by Sompolinsky to encode the anomalous response to a field perturbation at large time scales ($x < 1$, $x > 1$ in the parametric representation used so far). The anomaly function is a direct way to measure ergodicity breaking occurring in spin glasses (see Ref. 34,35), even at infinite time ($x = 0$). Defining the susceptibility function at the time-scale labeled by x as

$$\chi(x) = J [q(1)] + \chi(x); \quad (89)$$

where $\chi(x)$ is given by the stationarity Eq. (61), the equilibrium susceptibility, Eq. (86), can be rewritten as

$$\chi_0 = \chi(0) = J [q(1)] + \chi(0); \quad (90)$$

The anomaly $\chi(0)$ can, thus, be interpreted as the difference between the theoretical descriptions of the zero-field-cooled and the field-cooled susceptibility.

$$\begin{aligned} \chi(0) &= \chi(1) - \chi(0) = \int_0^1 dx q(x) - \int_1^{R_1} dy P(0;y) m^0(0;y) \\ &= (q_{EA} - \bar{q}): \end{aligned} \quad (91)$$

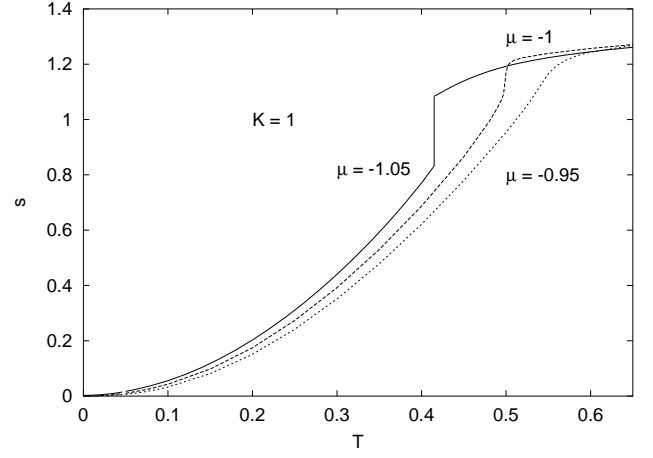


FIG. 5: Entropy density as a function of temperature for $K = J$. For $\mu < \mu_c = J$ the entropy is discontinuous at the transition temperature: a latent heat is produced/employed at the transition.

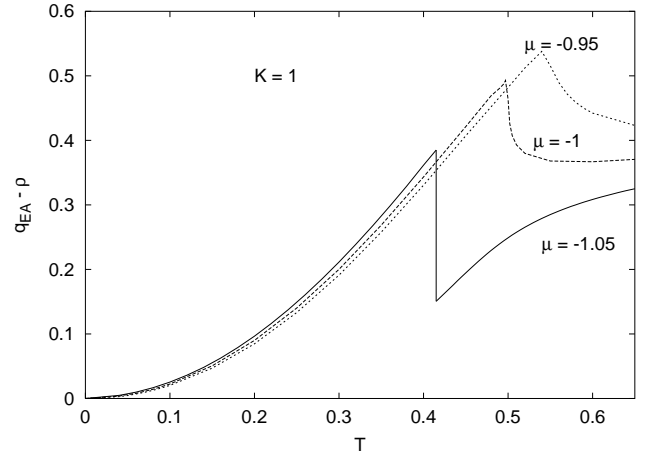


FIG. 6: $q(1)$ as a function of temperature for $K = J$. For $\mu < \mu_c = J$ there is a discontinuity at the transition temperature.

$$7. \text{ Free Energy Integral } \int_1^{R_1} dy P(0;y) m^0(0;y)$$

The often occurring integral $\int_1^{R_1} dy P(0;y) m^0(0;y)$ [see Eqs. (53) and (67)] can be expressed as a function of the local magnetization $m(0;y)$, numerically found as solution of coupled Eqs. (59), (64) $x = 0$. From the magnetization definition we write the identity

$$m(0;y) = m(0;0) + \int_0^1 dy^0 m^0(0;y^0); \quad (92)$$

that is valid for every y . Combining this with the identity $\int_1^{R_1} dy P(0;y) = \int_0^1 dx -q(x;y)$ and taking the limit

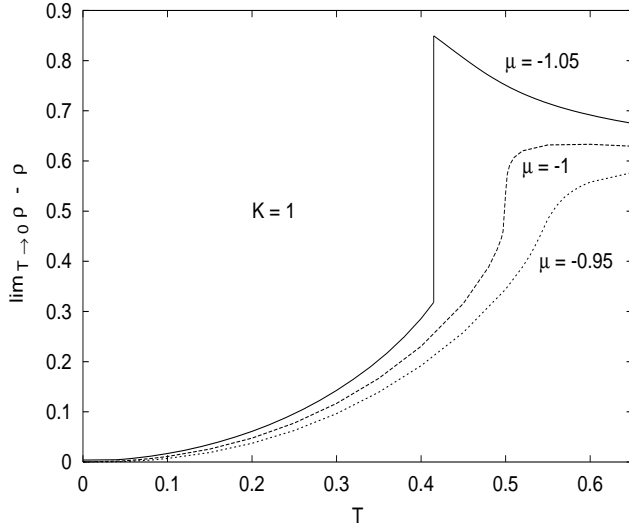


FIG. 7: m as a function of temperature for $K = J$. For $\mu < \mu_c = J^- < 1$ and there is a discontinuity at the transition temperature.

$y \in [0, 1]$, we get for the constant $(0; 0)$ the value

$$\begin{aligned} (0; 0) &= \lim_{y \rightarrow 1} T^{-1} + \int_0^1 \frac{1}{2} \frac{Z_1}{Z_y} dx - (x) \quad (93) \\ &= T^{-1} - \frac{1}{2} \int_0^1 \frac{Z_1}{Z_y} dx - (x) + \int_0^1 dy [1 - m(0; y)] : \end{aligned}$$

This leads to the more convenient expression, for a numerical computation,

$$\begin{aligned} &\int_0^1 dy P(0; y) - (0; y) \quad (94) \\ &= T^{-1} - \frac{1}{2} \int_0^1 \frac{Z_1}{Z_y} dx - (x) + \int_0^1 dy [1 - m(0; y)] \\ &\quad + \int_0^1 dy P(0; y) - dy^0 m(0; y^0) : \end{aligned}$$

A. Low Temperature Behavior in the FRSB SG Phase

From the self-consistency Eqs. (62-63) we can get the $T = 0$ limit of $q(1)$ and m . As in the RS case previously reported (see Sec. IIB), also for the stable solution that limit crucially depends from the sign of μ_1 at zero temperature. Once again we define $\mu_1(T) = (\mu/J)$ and we sketch the results in the two qualitatively different cases:

1. Full lattice at zero temperature: $\mu > 0$

For $T \rightarrow 0$ the last term of the entropy in Eq. (82) goes as

$$\begin{aligned} &\int_0^1 dy P(1; y) [1 - (1; y) - y m(1; y)] \quad (95) \\ &= -\rho(0) + O(e^{-1/T}) \end{aligned}$$

where the boundary functions $(1; y)$ and $m(1; y)$ are given by Eqs. (56, 65). The Edwards-Anderson parameter and the density both tend to one.

At zero temperature there is one single ground state and the entropy is, therefore, zero. So that, from Eq. (82), we get

$$0 = \lim_{T \rightarrow 0} \frac{(\mu/J)^2}{4} [q(1)^2 + (1 - \rho(0))] \quad (96)$$

Using Eq. (95) and equating the entropy expression at zero temperature to zero we see that $q(1)$ and ρ go to their $T = 0$ value in such a way that $q(1) \rightarrow 1$ and $\rho \rightarrow 1$ with $s; s^0 \rightarrow 1$.

To analytically determine the value of s and s^0 it turns out to be quite complicated. However, from our numerical computation, we find that, at low temperatures both the entropy and $q(1)$ reach the zero value as T^2 , thus $s = 2$. In order to satisfy formulas (82) and (99), then, ρ has to decrease as T^3 ($s^0 = 3$), also consistent with our numerical data.

2. Partially empty lattice: $\mu < 0$.

The parameter μ_1 tends to -1 at zero temperature and $q(1)$ and ρ are less than one, namely

$$\begin{aligned} \lim_{T \rightarrow 0} q(1) &= \lim_{T \rightarrow 0} \frac{Z_1}{Z_K} = 2 \int_0^1 dy P(1; y) \quad (97) \\ &= 2 \int_0^1 dy P(1; y) - K = J - J \end{aligned}$$

If $\mu_1 < 0$, in general, $e^{-1} \cosh Jy$ will not be much larger than one for any value of y in the argument of $(1; y)$ and in $y m(1; y)$. The zero T limit depends on the sign of μ_1 and $\mu_1 \neq 0$:

$$\lim_{T \rightarrow 0} (1; y) = \begin{cases} 1 & \text{if } y > 0 \\ \frac{T}{J} \log 2 & \text{if } y < 0 \end{cases} \quad (98)$$

The analogue of Eq. (95) is, in this case,

$$\begin{aligned} &\int_0^1 dy P(1; y) [1 - (1; y) - y m(1; y)] \quad (99) \\ &= (1 - \rho(0)) \log 2 + \rho(0) + O(e^{-1/T}) \end{aligned}$$

Since the zero temperature density is less than one, there will be a fraction $1 - \rho$ of spins whose orientation is irrelevant for measuring any observable. This brings to a degeneracy in the ground state, of $2^{N(1-\rho)}$ equivalent configurations. Then, for the entropy density, we get

$$s = \lim_{T \rightarrow 0} \frac{(-J)^2}{4} [\rho \ln \rho + (1-\rho) \ln (1-\rho)] + (1-\rho) \ln 2 \quad (100)$$

Also in this case we can see from numerical data at low temperature that the behavior of $q(1)$ and s is T^2 , whereas ρ is still consistent with our numerical data.

At zero temperature the free and internal energy are:

$$u = f = \frac{K}{2} \int_0^1 dx q(x) - (x) \quad (101)$$

where ρ is either 1 or ρ depending on the sign of μ .

V. PHASE DIAGRAMS

Analyzing the stability of the RS solution [see Eqs. (25,26)] one gets the critical lines

$$1 - (J)^2 = 0; \quad (102)$$

$$1 - K(1 - \rho) = 0; \quad (103)$$

above which the only solution is the PM solution $q(x) = 0$ for $x \in [0, 1]$, $\rho = 1/[1 + e^{-J}]$ [see Eq. (24)], stable for any value of K . In the T - ρ plane, these are, respectively, the straight line and the left branch of the spinodal line shown in Fig. 8, for $K = J$. The two lines meet at the tricritical point (29)–(30). Between them, under the two hard line curves branching out from the tricritical point, there is a region of coexistence of phases (as indicated in the plot of Fig. 8). The broken line curves are the first order transition lines. When $\mu < \mu_c$, in cooling at fixed chemical potential, the density of the system jumps discontinuously from the PM to the higher SG value. As an example the line at $\mu = -1.05$ is plotted.

By crossing the critical line Eq. (102) above the tricritical point ($\mu > \mu_c, T > T_c, \rho > \rho_c$) the system undergoes a continuous phase transition of the SK-type to a FRSB SG phase, with a non-trivial continuous order parameter function $q(x)$ which smoothly grows from zero.

Below the tricritical point the scenario is completely different, displaying a discontinuous transition from the PM phase to a FRSB SG phase with $q(x)$ which discontinuously jumps from zero to a non-trivial (continuous) function. At the critical temperature the entropy is discontinuous, see Fig. 5, and hence a latent heat is involved in the transformation from the PM to the SG phase, implying that the transition is of the first order in the thermodynamic sense. The transition line is determined by the free energy balance between the PM and

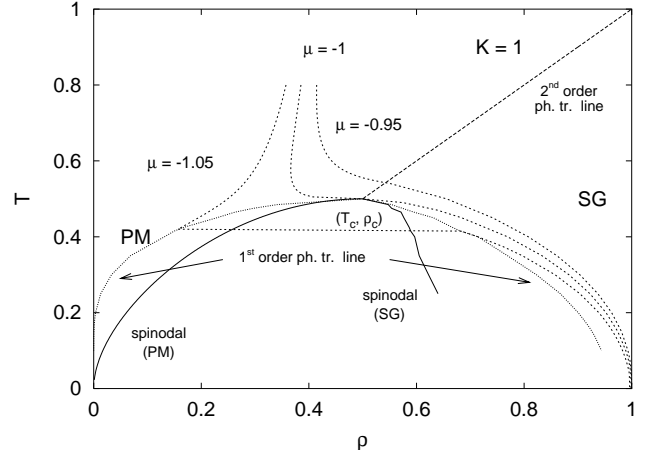


FIG. 8: T - ρ phase diagram of the RBEGC for $K=J=1$. The dot marks the tricritical point $\rho_c=J=1$, $T_c=J=2$, $\mu_c=1=2$. In the upper-left region we have the paramagnetic (PM) phase. In the upper-right region the FRSB spin glass (SG) phase. Following the iso-potential line at $\mu=J=1.05$ one sees the jump in density at the first order phase transition.

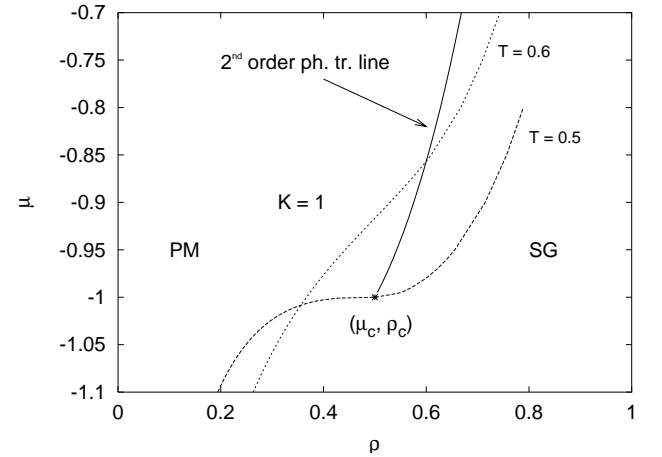


FIG. 9: μ - ρ phase diagram of the RBEGC for $K=1$. Above the tricritical point (star) the transition is second order. Two isothermal lines are shown for temperature $T=0.5; 0.6$, i.e. at and above.

the SG phase, and is shown as a broken line in the phase diagrams. The line yielded by Eq. (103) where the PM solution becomes unstable, and the equivalent line from the SG side are the spinodal lines.

Also interesting is the μ - ρ phase diagram represented in Figs. 9, 10. We indeed see that the isothermal lines cross the instability lines with vanishing derivative (Fig. 10) and hence a diverging compressibility occurs crossing these lines.

It can be shown that the first order transition line can be determined in the μ - ρ phase diagram from the isothermal and spinodal lines by using a Maxwell con-

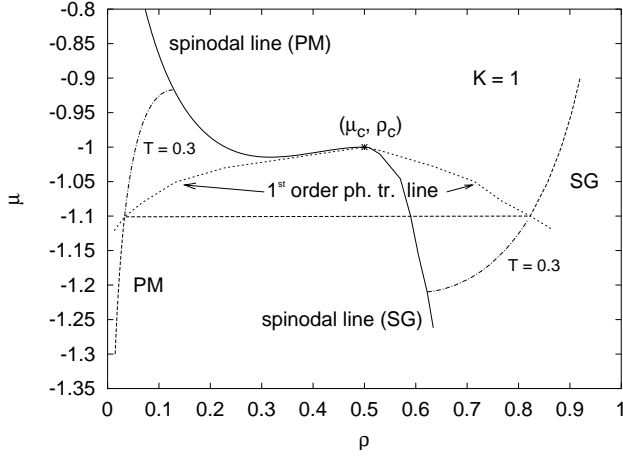


FIG. 10: μ - ρ phase diagram of the RBEGC for $K = 1$. From the tricritical point (star) two solid lines come out: the spinodal lines at which the paramagnetic (upper-left curve) and the spin glass (lower-right curve) phases cease to exist, even as metastable. The first order transition lines, also branching out of the tricritical point, are plotted as dashed curves. An isothermal line is shown, for a temperature $T = 0.3$ below $T_c = 1/2$. Along such curve a first order phase transition occurs. In the plot, also the metastable branches are shown, both in the RSPM phase and in the FRSG SG phase (broken curves continuing the full curves). They reach the spinodal lines with zero derivative. In this plane of conjugated thermodynamic variables a Maxwell construction can be explicitly performed.

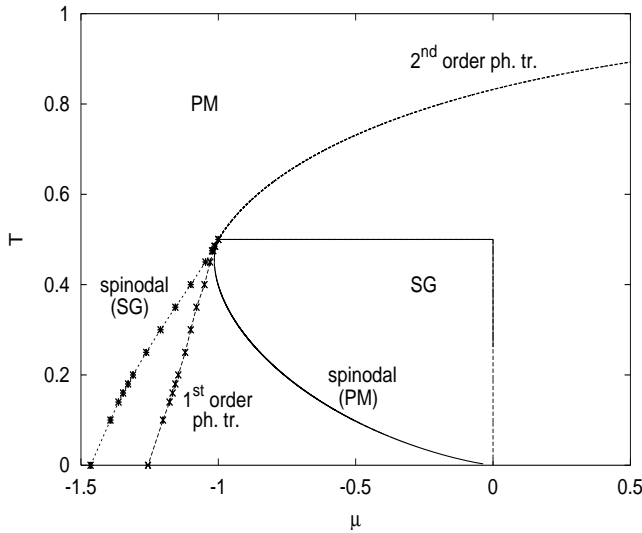


FIG. 11: T - μ phase diagram of the RBEGC for $K = 1$. For low μ (lower than -1.2 in this specific case) the code at $T = 0$ - in the Sommers gauge - is very unstable. Therefore the zero- T transition points are obtained by μ - ρ construction.

In the region between the first order transition line and the spinodal line the pure phase is metastable.

Below the spinodal lines (in the T - ρ plane) no pure phase can exist and the system is in a mixture of PM and SG phase (phase coexistence).

Eventually, the phase diagram in the T - ρ plane, for $K = 1$, is shown in Fig. 11. Since our code, even in 'most suitable' gauge (see Sec. IIIB), is unstable in region of both low temperature and low chemical potential we were not able to reliably compute the points belonging to the SG spinodal line and the first order phase transition line for $T < 0.1 = T_c/5$. The prolongation of the lines down to zero temperature are, hence, computed by μ - ρ . Therefore the zero- T transition are estimates rougher than the others. The first order line goes to $\rho_0^{1st} = 1.256 \pm 0.009$ and the spinodal one reaches zero at $\rho_0^{SG} = 1.465 \pm 0.008$. Nevertheless, it seems that we can rule out a reentrance to the PM phase as $T \rightarrow 0$.

By varying K the scenario remains qualitatively unchanged [look at Ref.¹⁵ for the phase diagrams of the Ghatik-Sherrington model¹⁸ ($K = 0$) and the frustrated Ising lattice gas model²² ($K = J$)]. The only effect of a strong repulsive particle-particle interaction is to increase the phase diagram zone where the empty system ($\rho = 0$) is the stable solution. In order to find further phases, e.g. an antiquadrupolar phase,²³ a generalization of the present analysis to a two component magnetic model,⁵³ including quenched disorder, has to be carried out.⁵⁰

If we now look at the qualitative reproduction of the phase diagram of the original BEG model, with ferromagnetic interaction, in Fig. 1 one can imagine a correspondence between the PM phase of the disordered magnetic material and the fluid phase of the He^3 - He^4 mixture, and between the SG phase and the superfluid phase. The density corresponds to the He^4 density and the density x of He^3 particles is 1. The second order transition line corresponds to the transition points from fluid to superfluid.

A. Transition Lines

The starting point to analytically determine the transition lines around the tricritical point is the expansion of Eq. (8) for small q and densities next to ρ_c that we report in appendix VI [Eq. (165)]. There the various coefficients are expressed in terms of the function $\phi_0 = (1 + \exp(-K/T))^{-1}$ coinciding with the paramagnetic density of the system evaluated along the second order transition line $\phi_0 = 0$ (along which is $\mu = \mu_0 = T/J$). The expansion parameters are the elements of the overlap matrix q_{ab} and r_0 (replica independent).

One can obtain the approximated analytical expression of the spinodal line at which the FRSG solution disappears and the first order transition line, at which the paramagnetic free energy overcomes the approximated spin glass free energy, around the tricritical point.

In figure 12 we show both the behavior of the spinodal

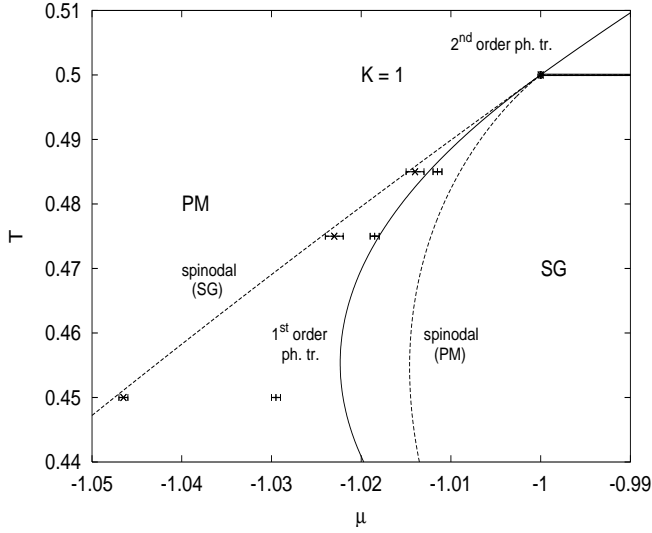


FIG. 12: The T - μ phase diagram around the tricritical point. The points displayed are those computed by directly solving the FRSB equations at given T and probing in μ where the SG solution disappears (SG spinodal) and when the SG free energy becomes lower than the PM one (1st order transition). The lines are obtained, instead, from the free energy expanded to the second order in T . Also the second order transition and the PM spinodal line are displayed.

line of the spin glass phase and the behavior of the 1st order transition line for the case $K = J$, in the neighborhood of the tricritical point in the T - μ plane. The points in the plot are obtained by numerically solving the FRSB differential equations. Notice that, at the order of approximation used, the 1st order line displays a reentrance that does not occur, instead, performing the exact computation.

Notice that, at the present degree of approximation, already at such small distance from $(\mu_c; T_c)$ the 1st order line displays a reentrance, whereas the exact computation shows that this does not take place.

In the following we consider $\mu = J$ and $T = J$. T and we express everything in terms of the small quantities ϵ , T and T and

$$\frac{\partial \phi_0(T)}{\partial T} T; \quad (104)$$

This last auxiliary variable represents the distance from the second order phase transition line. If $\epsilon < 0$, in the T - μ plane, we are above the second order line (PM phase), otherwise below (SG phase). The function $\phi_0(T)$ is defined as:

$$\phi_0(T) = \frac{1}{2} T K - T \log \frac{1}{T} - 1 \quad (105)$$

The expressions of $r = \phi_0$ and q_1 , the highest value of $q(x)$, are

$$q_1 = \frac{3}{2} T + \frac{1}{2} \frac{1}{T} \quad (106)$$

$$r = \frac{T}{2} + \frac{1}{2} \frac{1}{T} \quad (107)$$

Since T is always negative the above parameters are always positive, as far as they exist ($T < 0$). The solution breaks down at the spinodal line, therefore given by $\mu = T^2$, i.e.

$$\mu = \mu_c + T_c + T + (T - T_c)^2 \quad (108)$$

From the comparison of the free energy values for the PM and the SG phases the approximated 1st order transition line turns out to be

$$\mu = \mu_c + T_c + T + 11.19(T - T_c)^2 \quad (109)$$

VI. CONCLUSIONS

In the present paper we have shown, in some detail, the properties of the Random Blume-Emery-Griffiths-Capel model. Such a model can be seen both as a 1-spin model or a Ising-spin model on a lattice gas. The two formulations are completely equivalent, at least from a static point of view. In the second representation, that we adopted, the interactions involved are a quenched random magnetic coupling J_{ij} between spins and an attractive/repulsive coupling between (full) sites (K). The system is embedded in a reservoir and the exchange of particles is controlled by the chemical potential. The quenched random interaction is the source of a spin-glass phase at low temperature, provided that the chemical potential is large enough. If, on the contrary, μ is lower than a certain value, the system happens to be always in the paramagnetic phase, becoming progressively empty as $T \rightarrow 0$. We analytically studied the system in the mean field approximation. As already shown by the authors in Ref. [15] the qualitative features of the system do not depend of the value of K , nor on the coupling being repulsive, attractive or zero.

The external parameters are the temperature and the chemical potential. In a certain region of the phase diagram (see figure 11 in Sec. V) for the T - μ diagram at particle-particle interaction $K = J$, or, else, figures 8, 9 and 10) the system undergoes a second order transition varying T or μ , down to a given 'tricritical' point at which the second order line ends. Indeed, the main feature of this model is that for low temperature, or high chemical potential, a continuous transition (in the Ehrenfest sense) from a pure PM phase to a pure SG phase does not occur anymore. In its place a 1st order transition takes place, with consumption/production of latent heat (see Fig. 5 in Sec. IV) and the appearance of a region of the parameter space where the two phases (PM and SG) do coexist. The SG phase comes out to be stable exclusively in the FRSB scheme of computation. We can, thus, rule

out the existence of a glass-like phase, by this meaning a phase with one step RSB in the static, corresponding to a dynamical decoupling of the characteristic time scales of the processes involved in two time sectors. Only one kind of spin glass phase exist in the frozen phase and this is the one typical of mean-field models for amorphous systems (i.e. spin-glasses in the proper sense). In order to recover a system with a stable 1RSB phase and displaying a first order transition a lattice gas of spins interacting through multiple spins interaction (i.e. a p-spin spin glass on lattice gas) has to be considered (see e.g. Ref. [48]). It is interesting to notice that a discontinuous transition between liquid and glass, with coexistence of phases, has been recently found in lattice heteropolymers with random interactions^{46,47}. We also mention that generalizing the present model to a two component magnetic model⁵³, and including quenched disorder, further phases can be found, e.g. an antiquadrupolar phase.

Computing the state of the system down to very low temperature (including zero for not extremely low values) it has been possible to see that the reentrance displayed in the T - phase diagram in the Replica Symmetric approximation is just an artifact (see e.g. [20], but also the 'small q' expansion in Appendix B). There is no range for which lowering the temperature the spin glass can transform itself in a paramagnet.

We have discussed in detail the numerical method that we use to solve the antiparabolic differential Parisi equation for the present model, allowing us to compute the overlap order parameter and all the thermodynamic observables in the SG phase. In particular we face the problem of making the code converge at very low temperature, including zero. Section III is dedicated to the presentation and explanation of the variational approach to the problem of computing the FRSB antiparabolic differential equations and the pseudo-spectral method employed to solve them.

Besides the numerical resolution of the FRSB equations we have also studied the phase diagrams around the tricritical point making an expansion for small overlap values and densities next to the density at the tricritical point (see Sec. V A and appendix V I). The expansion formalism is valid all along, and around, the second order transition line. The only interesting point around which is worth probing the parameter space is, however, the tricritical point. From there one can build analytical approximated expressions for the spinodal line of the spin glass phase and for the first order transition line as well. Above the tricritical point the transition is always second order and qualitatively identical to the phase transition taking place in the Sherrington-Kirkpatrick model, that is easily recovered as limit of the present model (density one, zero chemical potential, full lattice).

APPENDIX A : Stability Analysis in the Replica Formalism

Rescaling $J \rightarrow J_0$, $J_0 = J$, $K = J$, $K = J$, $h = J$, $h = J$ and, consequently $K \rightarrow K$, $K = J$ we write the replica thermodynamic potential (8) as

$$G(f, g; f_m, g; f_{qg}) = -n \int \mathcal{D}(f, g; f_m, g; f_{qg}) \quad (110)$$

$$= \frac{K}{2} \sum_{a=1}^n X_a^2 + \frac{J_0}{2} \sum_{a=1}^n m_a^2 + \frac{1}{4} \sum_{a \neq b}^n X_a^2 X_b^2 q_{ab}^2 \log Z^0$$

with Z^0 and H^0 given respectively in Eqs. (9), (10) and repeated here for clarity:

$$Z^0 = \int \mathcal{D}(f, g; f_m, g; f_{qg}) \exp \left[-H^0[f, g; f_m, g; f_{qg}] \right] \quad (111)$$

$$H^0[f, g; f_m, g; f_{qg}] = \sum_a \left[\frac{K}{2} f_a^2 + \frac{J_0}{2} m_a^2 + \frac{1}{4} \sum_{a \neq b} X_a^2 X_b^2 q_{ab}^2 \right] \quad (112)$$

The variation of G with respect to the replica parameters is

$$G(f, g; f_m, g; f_{qg}) = \sum_a \left[\frac{K}{2} f_a^2 + \frac{J_0}{2} m_a^2 + \frac{1}{4} \sum_{a \neq b} X_a^2 X_b^2 q_{ab}^2 \right] \quad (113)$$

$$+ \sum_a \left[\frac{K}{2} f_a^2 + \frac{J_0}{2} m_a^2 + \frac{1}{4} \sum_{a \neq b} X_a^2 X_b^2 q_{ab}^2 \right] \quad (114)$$

$$+ \sum_a \left[\frac{K}{2} f_a^2 + \frac{J_0}{2} m_a^2 + \frac{1}{4} \sum_{a \neq b} X_a^2 X_b^2 q_{ab}^2 \right] \quad (115)$$

$$+ \sum_a \left[\frac{K}{2} f_a^2 + \frac{J_0}{2} m_a^2 + \frac{1}{4} \sum_{a \neq b} X_a^2 X_b^2 q_{ab}^2 \right] \quad (116)$$

where the average $\langle \cdot \rangle$ is performed with the measure given by Eq. (112). From G the saddle point equations are immediately derived:

$$q_{ab} = \langle f_a f_b \rangle \quad (114)$$

$$m_a = \langle f_a \rangle \quad (115)$$

$$m_a = \langle f_a \rangle \quad (116)$$

Eventually the fluctuations functional is equal to

$${}^2G(f, g; f_m, g; f_{qg}) = \sum_a \left[\frac{K}{2} f_a^2 + \frac{J_0}{2} m_a^2 + \frac{1}{4} \sum_{a \neq b} X_a^2 X_b^2 q_{ab}^2 \right] \quad (117)$$

$$+ \sum_a \left[\frac{K}{2} f_a^2 + \frac{J_0}{2} m_a^2 + \frac{1}{4} \sum_{a \neq b} X_a^2 X_b^2 q_{ab}^2 \right] \quad (118)$$

$$+ \sum_a \left[\frac{K}{2} f_a^2 + \frac{J_0}{2} m_a^2 + \frac{1}{4} \sum_{a \neq b} X_a^2 X_b^2 q_{ab}^2 \right] \quad (119)$$

$$+ \sum_a \left[\frac{K}{2} f_a^2 + \frac{J_0}{2} m_a^2 + \frac{1}{4} \sum_{a \neq b} X_a^2 X_b^2 q_{ab}^2 \right] \quad (120)$$

where

$$h_{a_1} :: o_{a_k} i = \frac{P_{fsg} o_{a_1} :: o_{a_k} e^{H^0}}{Z^0} \quad (118)$$

$$= h_{a_1} :: o_{a_k} (H^0) i \quad h_{a_1} :: o_{a_k} i h (H^0) i$$

and

$$(H^0) = K^n \sum_{a=1} n_a a \quad (119)$$

$$+ J_0 \sum_{a=1} S_a n_a m_a + \frac{1}{2} \sum_{a \neq b} S_a n_a S_b n_b q_{ab} :$$

In (117) we have, thus, six kinds of terms: the quadratic ones and the mixed ones whose coefficients are given in table II.

The functional 2G , that has to be definite positive in order for the solution around which the expansion is performed to be stable, takes the form

$${}^2G = \sum_{ab} (q_{ab})^2 + K \sum_a (a)^2 \quad (120)$$

$$+ J_0 \sum_a (m_a)^2 + \sum_{(ab);(cd)} q_{ab} A_{(ab)(cd)} q_{cd}$$

$$+ \sum_{(ab);c} q_{ab} D_{(ab)c} q_c + \sum_{(ab);c} q_{ab} E_{(ab)c} m_c$$

$$+ \sum_a D_a q_d + \sum_a B_{ac} q_c$$

$$+ \sum_a F_{ac} m_c + \sum_a E_a q_d$$

$$+ \sum_a F_{ac} q_c + \sum_a C_{ac} m_c ;$$

and the eigenvalues equations, then, come out to be

$${}^2 q_{ab} + \sum_{(ab);(cd)} A_{(ab)(cd)} q_{cd} \quad (121)$$

$$+ \sum_{(ab);c} D_{(ab)c} q_c + \sum_{(ab);c} E_{(ab)c} m_c = q_{ab} ; \quad (122)$$

$$K \sum_a q_a + \sum_a B_{ac} q_c + \sum_a F_{ac} m_c = a ; \quad (123)$$

$$J_0 \sum_a m_a + \sum_a E_a q_d + \sum_a F_{ac} q_c + \sum_a C_{ac} m_c = m_a ;$$

	Second order expansion term 2G
fluctuation term	coefficient
$q_{ab} q_d$	$A_{(ab)(cd)} = {}^4 (m_a S_a n_b S_b n_c S_c n_d S_d i - m_a S_a n_b S_b i m_c S_c n_d S_d i)$
$a c$	$B_{ac} = (K)^2 (m_a n_c i - m_a i m_c i)$
$m_a m_c$	$C_{ac} = (J_0)^2 (m_a S_a n_c S_c i - m_a S_a i m_c S_c i)$
$q_{ab} q_c$	$D_{(ab)c} = {}^3 K (m_a S_a n_b S_b n_c i - m_a S_a n_b S_b i m_c i)$
$q_{ab} m_c$	$E_{(ab)c} = {}^3 J_0 (m_a S_a n_b S_b n_c S_c i - m_a S_a n_b S_b i m_c S_c i)$
$a m_c$	$C_{ac} = {}^2 K J_0 (m_a n_c S_c i - m_a i m_c S_c i)$

TABLE II: Different contributions to the fluctuation functional of the Random BEG model in the replica formalism. All the averages have to be evaluated at the saddle point given by Eqs. (12)–(13). The subscript (ab) means distinct pairs of indexes.

A.1 The Stability of the RS Solution

Inserting in the above expressions the Ansatz that all replicas are equivalent (same density, same magnetization and same overlap between all of them) we can study

the stability of the RS solution. The RS Ansatz is implemented by the substitutions:

$$q_{ab} = (1 - \delta_{ab}) q_d ; \quad a = ; \quad m_a = m ; \quad (124)$$

	Replica Symmetric Expressions for the Coefficients in 2G	
$A_{(ab)(ab)} =$	${}^4 \ln_a n_b i \ln_a S_a n_b S_b i^2 = {}^4 \frac{R}{D_Y \sim^2(Y)} \frac{R}{D_Y m^2(Y)}^2$	$= A_2$
$A_{(ab)(ad)} =$	${}^4 \ln_a n_b S_b n_c S_c i \ln_a S_a n_b S_b i \ln_a S_a n_c S_c i = {}^4 \frac{R}{D_Y \sim(Y) m^2(Y)} \frac{R}{D_Y m^2(Y)}^2$	$= A_1$
$A_{(ab)(cd)} =$	${}^4 \ln_a S_a n_b S_b n_c S_c n_d S_d i \ln_a S_a n_b S_b i \ln_c S_c n_d S_d i = {}^4 \frac{R}{D_Y m^4(Y)} \frac{R}{D_Y m^2(Y)}^2$	$= A_0$
$B_{aa} =$	${}^2 K^2 \ln_a i \ln_a i m_b i = {}^2 K^2 \frac{R}{D_Y \sim(Y)} \frac{R}{D_Y \sim(Y)}^2$	$= B_1$
$B_{ac} =$	${}^2 K^2 \ln_a n_c i \ln_a i m_c i = {}^2 K^2 \frac{R}{D_Y \sim^2(Y)} \frac{R}{D_Y \sim(Y)}^2$	$= B_0$
$C_{aa} =$	${}^2 J_0^2 \ln_a i \ln_a S_a i^2 = {}^2 J_0^2 \frac{R}{D_Y \sim(Y)} \frac{R}{D_Y m(Y)}^2$	$= C_1$
$C_{ac} =$	${}^2 J_0^2 \ln_a S_a n_c S_c i \ln_a S_a i m_c S_c i = {}^2 J_0^2 \frac{R}{D_Y \sim^2(Y)} \frac{R}{D_Y m(Y)}^2$	$= C_0$
$D_{(ab)a} =$	${}^2 K \ln_a S_a n_b S_b i \ln_a S_a n_b S_b i m_a i = {}^2 K \frac{R}{D_Y m^2(Y)} \frac{R}{D_Y m^2(Y)} \frac{R}{D_Y \sim(Y)}$	$= D_1$
$D_{(ab)c} =$	${}^2 K \ln_a S_a n_b S_b n_c i \ln_a S_a n_b S_b i m_c i = {}^2 K \frac{R}{D_Y \sim(Y) m^2(Y)} \frac{R}{D_Y m^2(Y)} \frac{R}{D_Y \sim(Y)}$	$= D_0$
$E_{(ab)a} =$	${}^3 J_0 \ln_a n_b S_b i \ln_a S_a n_b S_b i m_a S_a i = {}^3 J_0 \frac{R}{D_Y \sim(Y) m(Y)} \frac{R}{D_Y m^2(Y)} \frac{R}{D_Y m(Y)}$	$= E_1$
$E_{(ab)c} =$	${}^3 J_0 \ln_a n_b S_b n_c S_c i \ln_a S_a n_b S_b i m_c S_c i = {}^3 J_0 \frac{R}{D_Y m^3(Y)} \frac{R}{D_Y m^2(Y)} \frac{R}{D_Y m(Y)}$	$= E_0$
$F_{aa} =$	${}^2 J_0 K \ln_a S_a i \ln_a i m_a S_a i = {}^2 J_0 K \frac{R}{D_Y m(Y)} \frac{R}{D_Y \sim(Y)} \frac{R}{D_Y m(Y)}$	$= F_1$
$F_{ac} =$	${}^2 J_0 K \ln_a n_c S_c i \ln_a i m_c S_c i = {}^2 J_0 K \frac{R}{D_Y \sim(Y) m(Y)} \frac{R}{D_Y \sim(Y)} \frac{R}{D_Y m(Y)}$	$= F_0$

TABLE III: Here we report the coefficients of the second order term in the expansion of the free energy functional (110) of the Random BEG C model around the RS solution. The left hand side of equalities shows the generic expression of the coefficients, whereas the right hand side gives the coefficients evaluated with the Ansatz of replica symmetry. On the far right column the abbreviation for the RS coefficients are listed.

Using the definition

$$\phi_0 = K + \frac{\phi_0}{2}; \quad (125)$$

the replica one site Hamiltonian (112) becomes:

$$H^0(\phi; m; \phi_0) = \sum_a n_a \ln_a S_a + (J_0 m + h) \sum_a n_a S_a + \frac{\phi_0}{2} \sum_a n_a S_a^2; \quad (126)$$

With this measure we have to compute the averages $\ln_{a_1} \dots \ln_{a_k}$ occurring in the saddle point equations (10)–(13) and in the coefficients of the eigenvalues equations (see Tab. II).

Opening", with the Hubbard-Stratonovic method, the squared sum in Eq. (126) into the Gaussian integral of an exponential with linear exponent we get

$$e^{-H^0} = \int_1^Z dY \exp \left(\sum_a Y \ln_a S_a \right); \quad (127)$$

with the one-index Hamiltonian

$$H_a(Y) = \phi_0 n_a + \tilde{R}(Y) n_a S_a \quad (128)$$

and

$$\tilde{R}(Y) = Y \frac{\phi_0}{2} + J_0 m + h; \quad (129)$$

We also define the one-index partition sum as

$$Z_a(Y) = \sum_{S_a, m_a} e^{-H_a(Y)} = 2 + 2 e^{-\phi_0} \cosh \tilde{R}(Y); \quad (130)$$

and the one-index average

$$\ln_{a_1} = \frac{\sum_{S_a, m_a} S_a m_a e^{-H_a(Y)}}{Z_a(Y)}; \quad (131)$$

that is a function of Y .

With the help of Eqs. (126), (128) we are now able to compute the numerator of the average $\ln_{a_1} \dots \ln_{a_k}$:

$$\sum_{S_{a_1} \dots S_{a_k}} e^{-H^0} \quad (132)$$

$$\begin{aligned} &= \int_1^Z dY \prod_{i=1}^k \left[\sum_{S_{a_i}, m_{a_i}} Y^{m_{a_i}} e^{-H_{a_i}(Y)} \right] \\ &= \int_1^Z dY [Z_1(Y)]^k \ln_{a_1} \dots \ln_{a_k}; \end{aligned} \quad (133)$$

so that the complete expression of the average is eventually given by:

$$\lim_{n \rightarrow 0} \langle \sigma_{a_1} \dots \sigma_{a_k} \rangle = \lim_{n \rightarrow 0} \frac{1}{Z^0} \int \prod_{i=1}^n dY_i [Z_1(Y)]^{Y_i^k} \sigma_{a_1} \dots \sigma_{a_k} \\ = \int \prod_{i=1}^n dY_i \sigma_{a_1} \dots \sigma_{a_k}; \quad (134)$$

since $Z^0 = \int \prod_{i=1}^{R_1} dY_i [Z_1(Y)]^{Y_i^1} \neq 1$ in the zero replicas limit.

In our case σ_a can be any combination of n_a and $n_a S_a$ occurring in Eqs. (114)–(116) and in the coefficients of the second order expansion term of the thermodynamic potential [Eq. (117)] reported in Tab. II. In Eq. (128) n_a is coupled to ϕ_0 , whereas $n_a S_a$ is coupled to $\tilde{\mu}$. Their one-index averages can, then, be obtained as:

$$\langle \sigma_a \rangle = \frac{\partial \log Z_a(Y)}{\partial \phi_0} = \frac{\cosh \tilde{\mu}(Y)}{e^{-\phi_0} + \cosh \tilde{\mu}(Y)} \sim(Y); \quad (135)$$

$$\langle \sigma_a S_a \rangle = \frac{\partial \log Z_a(Y)}{\partial \tilde{\mu}} = \frac{\sinh \tilde{\mu}(Y)}{e^{-\phi_0} + \cosh \tilde{\mu}(Y)} \sim(Y); \quad (136)$$

Using these results we get Eqs. (19)–(21) and the expression of the coefficients of 2G for the RS solution. We report the complete list in table III. Filling in those terms, the sum occurring in the eigenvalues Eqs. (121)–(123) can, thus, be written in the RS scheme as:

$$\sum_{(cd)} A_{(ab)(cd)} Q_d = (A_2 - 2A_1 + A_0) Q_b \quad (137)$$

$$+ (A_1 - A_0) \left(\sum_c Q_c + Q_c \right) + \frac{A_0}{2} \sum_{cd} Q_d \\ \sum_c D_{(ab)c} Q_c = (D_1 - D_0) (\phi_a + \phi_b) + D_0 \phi_c \quad (138)$$

$$\sum_c E_{(ab)c} m_c = (E_1 - E_0) (m_a + m_b) + E_0 m_c \quad (139)$$

$$\sum_{(cd)} D_{a(cd)} Q_d = (D_1 - D_0) \sum_c Q_c + \frac{D_0}{2} \sum_{cd} Q_d \quad (140)$$

$$\sum_c B_{ac} Q_c = (B_1 - B_0) \phi_a + B_0 \phi_c \quad (141)$$

$$\sum_c F_{ac} m_c = (F_1 - F_0) m_a + F_0 m_c \quad (142)$$

$$\sum_{(cd)} E_{a(cd)} Q_d = (E_1 - E_0) \sum_c Q_c + \frac{E_0}{2} \sum_{cd} Q_d \quad (143)$$

$$\sum_c F_{ac} Q_c = (F_1 - F_0) \phi_a + F_0 \phi_c \quad (144)$$

$$\sum_c C_{ac} m_c = (C_1 - C_0) m_a + C_0 m_c \quad (145)$$

In the case $J_0 = 0$ (no ferromagnetic phase) $C_{ab} = E_{(ab)c} = F_{ab} = 0$, $8a; b; c$ and we are left with a system of equations for $n(n-1)=2$ variables Q_b and n variables ϕ_a (m_a are not involved, since always coupled with J_0). In total, the dimension of the space of solutions is $d_{\text{tot}} = n(n+1)=2$.

To obtain the first eigenvalue ϕ_0 we analyze the equations (121)–(122) in the subspace

$$\sum_a Q_b = 0; \quad 8b; \quad \phi_a = 0; \quad 8b; \quad (146)$$

These are $2n$ equations and the dimension of this subspace is $d_0 = d_{\text{tot}} - 2n = n(n-3)=2$, corresponding to the degeneracy of ϕ_0 . Eq. (146) also implies that $\sum_{ab} Q_b = \phi_a = 0$.

Using the conditions (146), the equations (121), (122) are easily reduced, in this case, to the single equation

$$(\phi^2 + A_2 - 2A_1 + A_0) Q_b = 0 \quad Q_b; \quad (147)$$

yielding

$$\phi_0 = \phi^2 + A_2 - 2A_1 + A_0; \quad (148)$$

We look at the second eigenvalue in the subspace

$$\sum_{ab} Q_b = 0; \quad \phi_a = 0; \quad (149)$$

where, as opposed to the previous case, $\phi_a \neq 0$, $8b$ and $\phi_a \neq 0$, $8a$. The ϕ_0 and the ϕ_1 subspaces are orthogonal.

Subtracting two [the equalities given in Eq. (149)] and the degeneracy of the ϕ_0 to the total dimension we get the degeneracy of ϕ_1 : $d_1 = d_{\text{tot}} - d_0 - 2 = 2(n-1)$.

Eqs. (121)–(122) reduce in this subspace to

$$(\phi^2 + A_2 + (n-4)A_1 - (n-3)A_0) Q_b \quad (150)$$

$$+ (n-2)(D_1 - D_0) \phi_a = \phi_1 Q_b \\ (D_1 - D_0) \sum_b Q_b \\ + (K + B_1 - B_0) \phi_a = \phi_1 \phi_a \quad (151)$$

for which the eigenvalue comes out to be

$$\epsilon_1 = \frac{1}{2} h^2 + A_2 + \frac{(n-4)A_1 + (n-3)A_0 + K + B_1 + B_0}{\frac{1}{2} h^2 + A_2 + (n-4)A_1 + (n-3)A_0 + (K + B_1 + B_0) + 4(n-2)(D_1 + D_0)^2} \quad (152)$$

To find ϵ_2 we are left with the subspace of solutions such that

$$q_{ab} = 0; \quad q_a = 0: \quad (153)$$

and whose dimension is 2.

The eigenvalue equations become now

$$\frac{1}{2} h^2 + A_2 + (n-2)2A_1 + \frac{n-3}{2}A_0 \quad q_{ab}$$

$$+ (n-1)[2D_1 + (n-2)D_0] \quad q_a = \frac{1}{2} h^2 + A_2 + A_{ab} \quad (154)$$

$$D_1 + \frac{n-2}{2}D_0 \quad q_{ab} \quad (155)$$

$$+ K + B_1 + (n-1)B_0 \quad q_a = \frac{1}{2} h^2 + A_2 + A_a$$

so that it, finally, holds

$$\epsilon_2 = \frac{1}{2} h^2 + A_2 + 2(n-2)A_1 + \frac{(n-2)(n-3)}{2}A_0 + D_1 + \frac{n-2}{2}D_0 \quad (156)$$

$$\frac{1}{2} h^2 + A_2 + (n-2)2A_1 + \frac{n-3}{2}A_0 \quad D_1 + \frac{n-2}{2}D_0 + 2(n-1)[2D_1 + (n-2)D_0]^2$$

In the limit for $n \rightarrow 0$ the eigenvalues ϵ_1 (152) and ϵ_2 (156) are degenerate. They reduce both to

$$\epsilon_1 = \epsilon_2 = \frac{1}{2} h^2 + A_2 + \frac{4A_1 + 3A_0 + K + B_1 + B_0}{\frac{1}{2} h^2 + A_2 + 4A_1 + 3A_0 + K + B_1 + B_0 + 8(D_1 + D_0)^2} \quad (157)$$

If we also put $h = 0$ we simplify things much, since in this case the stable solution is $q_0 = 0$. This brings to

$$\chi(y) = \frac{1}{e^{y_0} + 1} \quad (158)$$

$$\chi(y) = 0; \quad (159)$$

and, therefore, no integral in the coefficients of table III has to be carried out anymore. This leads to $A_1 = A_0 = D_1 = D_0 = B_0 = 0$ and

$$A_2 = \frac{4}{3} \quad (160)$$

$$B_1 = K^2 \quad (161)$$

Substituting these coefficients into Eqs. (148)–(157) we

obtain

$$\epsilon_0 = \frac{1}{2} h^2 + A_2 + A_0; \quad (162)$$

$$\epsilon_1 = K + 1 + K_0(1 - \epsilon_0); \quad (163)$$

The above analysis is valid for $K > 0$. This is always the case if the biquadratic coupling is $K > 0$. When a negative K occurs, however, at high enough temperature ($T > 1/(2K)$) K becomes negative. Taking this into account and repeating the whole scheme of computation the final result for $K < 0$ is, in the case of our interest,

$$\epsilon_1 = \frac{h}{K + 1 + K_0(1 - \epsilon_0)} \quad (164)$$

APPENDIX B : Small q Expansion

The expansion to the fourth order in $r = 0$ and q_{ab} is:

$$\begin{aligned}
 f(q_{ab}; r) = & f_0 + \frac{K}{J} r + \frac{1}{2} r^2 \frac{(K/J)^3}{6} (1 - 0) (1 - 2_0) r^3 \\
 & \frac{(K/J)^4}{24} (1 - 7_0 + 12_2 - 6^3) r^4 \\
 & + \frac{0}{4} \frac{1}{n} \text{Tr} q^2 + \frac{(J)^4}{2} K^2_0 (1 - 0) \\
 & r + \frac{K}{2} (2 - 3_0) r^2 + \frac{1}{n} \text{Tr} q^2 \\
 & \frac{(J)^6}{6} \frac{3}{2} \frac{1}{n} + 3 \frac{K}{J} (1 - 0) r + \frac{1}{n} \text{Tr} q^3 \\
 & \frac{(J)^8}{48} \frac{2}{n} \frac{1}{4} X_{habi} q_{ab}^4 + 6 \frac{X}{0} q_{ab}^2 q_{ac}^2 \\
 & + \frac{3}{2} \frac{X}{2} q_{ab}^2 q_{cd}^2 + 6 \frac{X}{0} q_{ab} q_{bc} q_{cd} q_{da}^5
 \end{aligned} \quad (165)$$

where $\sum_{h::i}$ is a sum over distinct indexes. The paramagnetic contribution is

$$f_0 = \frac{K}{2} + \log(1 - 0) \quad (166)$$

and

$$0 = \frac{1}{1 + \exp \frac{1}{K T = J}} \quad (167)$$

is the value of the paramagnetic density evaluated along the second order phase transition line.

The above expansion is valid in the neighborhood of the second order transition line, $0 = 0$, down to, and including the tricritical point ($0 = 0$ [$1 = 0$]).

The various terms appearing in the expansion of the free energy functional, Eq. (165) are expressed in the following. In order to compute it in a generic $N_B \rightarrow RSB$ scheme we just need the following expression for the form of the overlap matrix q_{ab}

$$q_{ab} = \frac{1}{N_B} \sum_{i=1}^{N_B} (q_i - q_1)_{ab}^{(i)} + q_0 \quad (168)$$

$$= \frac{1}{N_B} \sum_{i=1}^{N_B} (q_i - q_1)_{ab}^{(i)} \quad (169)$$

$$= \frac{1}{N_B} \sum_{i=1}^{N_B} q_i^{(i)}_{ab} \quad (170)$$

with $q_{N_B+1} = q_1 = 0$, $m_{N_B+1} = 1$, $m_0 = n$, $\frac{N+1}{ab} = \frac{N}{ab}$, $\frac{(0)}{ab}$ a $n \times n$ matrix with all elements equal to 1.

The matrix $\frac{(i)}{ab}$ has m_i blocks along the diagonal and its summation rules are:

$$X_{ab}^{(i)} = m_{\max(i,j)} \frac{m_{\min(i,j)}}{ac} \quad (171)$$

$$X_{ab}^{(j)} = \frac{(j)}{ac} \quad (172)$$

$$X_{ab}^{(i)} = m_i \quad (173)$$

$$X_{ab}^{(i)(j)(k)} = m_{\max(i,j,k)} \frac{m_{\min(i,j,k)}}{ad} \quad (174)$$

$$X_{ab}^{(i)(j)(k)(l)} = m_{\max(i,j,k,l)} \frac{m_{\min(i,j,k,l)}}{ae} \quad (175)$$

where $\sum_{:::}$ is a sum over all indexes.

$$\text{Term } \text{Tr} q^2 = \sum_{ab} q_{ab} q_{ba}$$

$$X_{ab} q_{bc} = \sum_{i=0}^{N_B} q_i^2 m_i \frac{(i)}{ac} m_{i+1} \frac{(i+1)}{ac} ; \quad (176)$$

$$X_{ab} q_{ba} = \sum_{i=0}^{N_B} q_i^2 (m_i - m_{i+1}) : \quad (177)$$

In the full replica symmetry breaking limit and in the zero replicas limit the breaking parameters become continuous between 0 and 1:

$$m_i \rightarrow i, m_k \rightarrow k, m_{i+1} \rightarrow i+1, dx : \quad (178)$$

Moreover the same structure of Eq. (177) holds for any $\frac{p}{ab}$, thus

$$\lim_{n \rightarrow 0} \frac{1}{n} \sum_{ab} q_{ab}^p = \lim_{n \rightarrow 0} \sum_{i=0}^{N_B} q_i^p (m_i - m_{i+1}) = \int_0^1 dx q^p(x) \quad (179)$$

type of sum	contribution	multiplicity
A : $i < j < k$	0	6
B : $i = j < k$	$q_k q_i^2 (m_k - m_{k+1}) (m_i - m_{i+1})$	3
C : $i < j = k$	0	3
D : $i = j = k$	$q_k^3 (m_k - m_{k+1})^2 - m_{k+1} (m_k - m_{k+1})$	1

TABLE IV : Contributions to the trace of q^3 for a generic number of breakings of the replica symmetry: only two kind of terms are different from zero.

$$\text{Term Tr} q^3 = \sum_{abc} q_{ab} q_{bc} q_{ca}$$

Using (170) this trace can be written as:

$$\begin{aligned} & \sum_{bc} \left[\sum_{(i)(j)(k)} \binom{(i)(j)(k)}{ab \ bc \ ca} + \sum_{(i)(j)(k)} \binom{(i+1)(j)(k)}{ab \ bc \ ca} + \sum_{(i)(j+1)(k)} \binom{(i)(j+1)(k)}{ab \ bc \ ca} + \sum_{(i+1)(j+1)(k)} \binom{(i+1)(j+1)(k)}{ab \ bc \ ca} \right] \\ & + \sum_{(i)(j)(k+1)} \binom{(i)(j)(k+1)}{ab \ bc \ ca} + \sum_{(i+1)(j)(k+1)} \binom{(i+1)(j)(k+1)}{ab \ bc \ ca} + \sum_{(i)(j+1)(k+1)} \binom{(i)(j+1)(k+1)}{ab \ bc \ ca} + \sum_{(i+1)(j+1)(k+1)} \binom{(i+1)(j+1)(k+1)}{ab \ bc \ ca} \end{aligned} \quad (180)$$

In table IV we report the four possible non degenerate contributions coming out from this sum and their multiplicity. In the full replica symmetry breaking limit (and for number of replicas $n \rightarrow 0$):

$$\begin{aligned} m_k! & \times \int_0^1 dx \, q(x)^2; \\ m_i! & \times \int_0^1 dy \, q(y)^2; \end{aligned}$$

Thus the above expressions for the terms contributing to the sum reduce to

$$B = \int_0^1 dx \, q(x)^2 + \int_0^1 dy \, q(y)^2; \quad (181)$$

$$D = \int_0^1 dx \, x \, q(x)^3; \quad (182)$$

where we have neglected terms of order $(dx)^2$. Summing up, the trace comes out to be:

$$\begin{aligned} \lim_{n \rightarrow 0} \frac{1}{n} \text{Tr} q^3 &= 3B + D \\ &= 3 \int_0^1 dx \, q(x)^2 + \int_0^1 dy \, q(y)^2 + \int_0^1 dx \, x \, q(x)^3 \end{aligned} \quad (183)$$

$$\text{Term Tr} q^4 = \sum_{abcd} q_{ab} q_{bc} q_{cd} q_{da}$$

Exploiting the formulation of Eq. (190) once again we can obtain

$$\begin{aligned} \sum_{bcd} q_{ab} q_{bc} q_{cd} q_{da} &= \sum_{i,j,k} q_i q_j q_k q_l \sum_{bcd} \left[\binom{(i)(j)(k)(l)}{ab \ bc \ cd \ da} + \binom{(i+1)(j)(k)(l)}{ab \ bc \ cd \ da} + \binom{(i)(j+1)(k)(l)}{ab \ bc \ cd \ da} + \binom{(i)(j)(k+1)(l)}{ab \ bc \ cd \ da} \right] \\ &+ \sum_{bcd} \left[\binom{(i)(j)(k)(l+1)}{ab \ bc \ cd \ da} + \binom{(i+1)(j+1)(k)(l)}{ab \ bc \ cd \ da} + \binom{(i+1)(j)(k+1)(l)}{ab \ bc \ cd \ da} + \binom{(i+1)(j)(k)(l+1)}{ab \ bc \ cd \ da} \right] \\ &+ \sum_{bcd} \left[\binom{(i)(j+1)(k+1)(l)}{ab \ bc \ cd \ da} + \binom{(i)(j+1)(k)(l+1)}{ab \ bc \ cd \ da} + \binom{(i)(j)(k+1)(l+1)}{ab \ bc \ cd \ da} + \binom{(i+1)(j+1)(k+1)(l)}{ab \ bc \ cd \ da} \right] \\ &+ \sum_{bcd} \left[\binom{(i+1)(j+1)(k)(l+1)}{ab \ bc \ cd \ da} + \binom{(i+1)(j)(k+1)(l+1)}{ab \ bc \ cd \ da} + \binom{(i)(j+1)(k+1)(l+1)}{ab \ bc \ cd \ da} + \binom{(i+1)(j+1)(k+1)(l+1)}{ab \ bc \ cd \ da} \right] \end{aligned}$$

Contribution and multiplicity are reported in table V.

For $N_B \rightarrow 1$ and $n \rightarrow 0$ the terms are

$$B = \int_0^1 dx \, q(x)^2 + \int_0^1 dy \, q(y)^2 + \int_0^1 dz \, z \, q(z)^3 \quad (184)$$

type of sum	contribution	m u l t i p l i c i t y
A : $i < j < k < l$	0	24
B : $i = j < k < l$	$q_l q_k q_i^2 (m_{l+1} - m_{l+1}) (m_k - m_{k+1}) (m_i - m_{i+1})$	12
C : $i < j = k < l$	0	12
D : $i < j < k = l$	0	12
E : $i = j < k = l$	$q_l^2 q_k^2 (m_k - m_{k+1})^2 (m_i - m_{i+1})$	6
F : $i = j = k < l$	$q_l q_k^3 (m_{l+1} - m_{l+1}) (m_k - m_{k+1})^2 m_{k+1} (m_k - m_{k+1})$	4
G : $i < j = k = l$	0	4
H : $i = j = k = l$	$q_l^4 (m_i - m_{i+1}) m_{i+1}^2 m_{i+1} (m_i - m_{i+1}) + (m_i - m_{i+1})^2$	1

TABLE V : Contributions and multiplicities of the terms in the sum of Eq. (184). Only for kinds of terms are non-zero. Of them, term E turns to be of order $(dx)^2$ once the zero replica limit has been performed.

$$E \neq 0 \quad (185)$$

$$F \neq \int_0^1 dx q(x) \int_0^1 dy y q^3(y) \quad (186)$$

$$H \neq \int_0^1 dx x^2 q^4(x) \quad (187)$$

$$\text{Term } P_{abc} q_{ab}^2 q_{ac}^2$$

Eventually this last object reads:

$$\begin{aligned} X_{bc} q_{ab}^2 q_{ac}^2 &= X_{ab} q_{ab}^2 q_{ac}^2 \\ &= \int_i q_i^2 (m_i - m_{i+1}) \int_j q_j^2 (m_j - m_{j+1}) ; \end{aligned} \quad (188)$$

the FRSB limit (for $n \rightarrow 0$) being

$$\begin{aligned} \lim_{n \rightarrow 0} \frac{1}{n} \int_{abc} q_{ab}^2 q_{ac}^2 &= \int_0^1 dx q^2(x) = 2 \int_0^1 dx q^2(x) \int_0^1 dy q^2(y) : \end{aligned} \quad (189)$$

1. Full RSB free energy for disordered BEG around T_c

Computing the expansion for small q and $r \rightarrow 0$, Eq. (165), in the FRSB scheme, yields

$$\begin{aligned} f &= f_0 - K \int_0^1 \frac{T}{J} \int_0^1 dx q(x)^2 \\ &+ \frac{1}{2} r^2 \frac{(K')^3}{6} \int_0^1 (1 - \rho) (1 - 2\rho) r^3 \\ &\frac{(K')^4}{24} \int_0^1 (1 - \rho) (1 - 6\rho + 6\rho^2) r^4 \\ &+ \frac{(J)^4}{2} K^2 \int_0^1 (1 - \rho) r + \frac{K}{2} (2 - 3\rho) r^2 \int_0^1 dx q(x)^2 \\ &\frac{(J)^6}{6} \int_0^1 1 + 3K \int_0^1 (1 - \rho) r \int_0^1 dx q(x) \int_0^1 dy q(y)^2 \end{aligned} \quad (190)$$

$$\begin{aligned} &+ \int_0^1 dx x q(x)^3 \\ &+ \frac{(J)^8}{8} \int_0^1 \int_0^1 dx q(x) \int_0^1 dy q(y) \int_0^1 dz q(z)^2 \\ &+ 4 \int_0^1 dx q(x) \int_0^1 dy y q(y)^3 + \int_0^1 dx x^2 q^4(x) \\ &+ \frac{(J)^8}{48} \int_0^1 (1 - 3\rho)^2 \int_0^1 dx q(x)^4 \\ &\frac{(J)^8}{8} \int_0^1 (1 - 3\rho) \int_0^1 dx q^2(x) \\ &+ \frac{(J)^{12}}{1440} \int_0^1 1 - 30\rho + 285 \int_0^1 \int_0^1 \int_0^1 \\ &+ 900 \int_0^1 \int_0^1 dx q^6(x) \end{aligned}$$

The expansion is valid along the critical line $T = T_c$ down to the tricritical point $(\rho_c; T_c)$ given by Eqs. (29–30).

The last term is introduced for the case $K = 0$, i.e. for the Gatak-Sherrington model, in which $1 - 3\rho$ goes to zero at the tricritical point $\rho_c = 1/3$ (e.g., decreasing temperature or density along the second order line). In this case the relevant quartic term $\int_0^1 dx q(x)^4$, responsible for the replica symmetry breaking, vanishes. This means that, in this case, the symmetry breaking is weaker than, for instance, in the SK case.

Putting $\rho = 1$ and $r = 0$ in the above expression we obtain the same result of Ref. [51], where the same kind of expansion for SK model is performed, up to the fourth order. To allow a straightforward check we rewrite the above formula in the way of Ref. [51]

$$\begin{aligned} f &= f_0 \\ &\frac{(J)^2}{4} \int_0^1 (1 - \rho) \int_0^1 dx q(x)^2 \\ &\frac{(J)^6}{6} \int_0^1 \int_0^1 dx x q(x)^3 + 3q(x) \int_0^1 dy q(y)^2 \\ &+ \frac{(J)^8}{24} \int_0^1 dx \left(3 \int_0^1 x^2 + \frac{1}{2} \int_0^1 (1 - 3\rho)^2 \right) q(x)^4 \end{aligned} \quad (191)$$

$$\begin{aligned}
& 2 \int_0^3 (1 - \frac{3}{2} y) q(x)^2 dy q(y)^2 \\
& + 12 \int_0^4 q(x) \int_0^x dy y q(y)^3 \\
& + 36 \int_0^4 q(x) \int_0^x dy q(y) \int_0^y dz q(z)^2 \\
& + O(q^6) + O(r)
\end{aligned}$$

Variation with respect to $q(x)$ and further differentiation with respect to x lead to an integralequation that can be reduced to

$$\frac{\partial_x q(x; r)}{q(x; r)} = \frac{1}{x} - \frac{6x^2}{(1 - \frac{3}{2}r + 6x^2)} \quad (192)$$

or

$$\partial_x q(x; r) = 0 \quad (193)$$

Below the critical temperature the solution is:

$$q(x; r) = \frac{C_1}{(1 - \frac{3}{2}r)} \frac{x}{(1 - \frac{3}{2}r + 6^2 x^2)} \quad (194)$$

as far as $x < x_M(r)$, otherwise $q(x; r) = q_1$ for $x > x_M(r)$. The value x_M is given by equating $q_1 = q(x_M; r)$:

$$x_M(r) = \sqrt{\frac{q_1(1 - \frac{3}{2}r)}{C_1^2 - 6^2(1 - \frac{3}{2}r)q_1^2}} + \frac{q_1(1 - \frac{3}{2}r)}{C_1} + O(r^3) \quad (195)$$

Notice that in Eqs. (192), (195) $r = r_0 + r$ and the formulas have yet to be expanded in r . The above computation can be simplified neglecting the quartic terms in Eq. (165) which are irrelevant with respect to the RSB, i.e. all but the one involving q_{ab}^4 . In this case $q(x)$ is simply

$$q(x) = A(r) x \quad (196)$$

with

$$A(r) = \frac{2}{(1 - \frac{3}{2}r)^2} + K(r)^6 \frac{(1 - \frac{3}{2}r)}{(1 - \frac{3}{2}r)^2} r \quad (197)$$

for $x < x_M$ $q=A(r)$ and $q(x) = q_1$ for $x > x_M$. If $r \rightarrow 0$ and $r_0 \rightarrow 1$ $A(0)$ reduces to $1=2$ (SK model).⁵²

- ¹ G. Parisi, J. Phys. A 13 (1980) L115.
- ² D. Sherrington, and S. Kirkpatrick, Phys. Rev. Lett. 26 (1975) 1782.
- ³ B. Derrida, Phys. Rev. Lett. 45 (1980) 79.
- ⁴ S.F. Edwards and P.W. Anderson, J. Phys. F 5 (1975) 965.
- ⁵ D.J.Gross, I.Kanter and h. Sompolinsky, Phys. Rev. Lett. 55 (1985) 305.
- ⁶ A. Crisanti and H.J. Sommers, Z. Phys. B 87 (1992) 341.
- ⁷ Th.M. Nieuwenhuizen, Phys. Rev. Lett. 74, 4289 (1995).
- ⁸ A. Crisanti and S. Ciuichi, Europhys. Lett. 9, 754 (2000).
- ⁹ P.M. Goldbart and D. Sherrington, J. Phys. C 18, 1923 (1985); P.M. Goldbart and Eldereld, J. Phys. C 18, L229 (1985); D. Sherrington, Prog. Theor. Phys. Supp. 87, 180 (1986).
- ¹⁰ E. Gardner, Nucl. Phys. B 257 (1985) 747.
- ¹¹ T.R. Kirkpatrick and P.G. Wolynes, Phys. Rev. A 35 (1987) 3072.
- ¹² D.J.Gross, M. Mezard, Nucl. Phys. B 240 (1984) 431.
- ¹³ J. P. Bouchaud, L. Cugliandolo, J. Kurchan and M. Mezard, in Spin Glasses and Random Fields, A. P. Young, ed. (World Scientific, Singapore, 1998), p. 161.
- ¹⁴ A. Crisanti, H. Hømer, H. J. Sommers, Z. Phys. B 92 (1993) 257.
- ¹⁵ A. Crisanti and L. Leuzzi, Phys. Rev. Lett. 89 (2002) 237204.
- ¹⁶ H.W. Capel, Physica 32, 966 (1966); M. Blume, Phys. Rev. 141, 517 (1966); M. Blume, V.J. Emery and R.B. Griffiths, Phys. Rev. A 4 (1971) 1071.
- ¹⁷ W. Hoston, A.N. Berker, Phys. Rev. Lett. 67 (1991) 1027.
- ¹⁸ S.K. Ghatak, D. Sherrington, J. Phys. C: Solid State Phys. 10, 3149 (1977).
- ¹⁹ E.J.S. Lage and J.R.L. de Almeida, J. Phys. C: Solid State Phys. 15 (1982) L1187.
- ²⁰ P.J.Mottishaw and D. Sherrington, J. Phys. C: Solid State Phys. 18 (1985) 5201.
- ²¹ F.A. da Costa, C.S.O. Yokoi and R.A. Salinas, J. Phys. A: Math. Gen. 27 (1994) 3365.
- ²² J.J. Arenzon, M. Nicodemi and M. Sellitto, J. Phys. I France 6 (1996) 1143.
- ²³ M. Sellitto, M. Nicodemi, J.J. Arenzon, J. Phys. I (France) 7 (1997) 945.
- ²⁴ F.A. da Costa, F.D. Nobre and C.S.O. Yokoi, J. Phys. A: Math. Gen. 30 (1997) 2317.
- ²⁵ G.R. Schreiber, Eur. Phys. J. B, 9 (1999) 479.
- ²⁶ F.A. da Costa, J.M. de Araujo, Eur. Phys. J. B, 15 (2000) 313.
- ²⁷ A. Aibino Jr., F.D. Nobre, F.A. da Costa, J. Phys.: Cond. Matt. 12 (2000) 5713.
- ²⁸ J.M. de Araujo, F.A. da Costa, F.D. Nobre, Eur. Phys. J. B, 14 (2000) 661.
- ²⁹ A. Caiazzo, A. Coniglio and M. Nicodemi, Phys. Rev. E 66, 046101 (2002).
- ³⁰ A. Caiazzo, A. Coniglio and M. Nicodemi, cond-mat 0311442
- ³¹ A. Coniglio, J. Phys. IV France 3 (1993) C1-1; Il Nuovo Cimento D 16 (1994) 1027.
- ³² A. de Candia and A. Coniglio, Phys. Rev. E 65, 16132 (2001).
- ³³ M. Nicodemi and A. Coniglio, Phys. Rev. E, 57, R39 (1998).
- ³⁴ M. Mezard, G. Parisi and M. Virasoro, Spin Glass Theory and Beyond (World Scientific, Singapore, 1987).
- ³⁵ K.H. Fischer and J.A. Hertz, Spin Glasses
- ³⁶ C. de Dominicis, M. Gabay and H. Orland, J. Phys. Lett. 42 (1981) L523.
- ³⁷ C. de Dominicis, M. Gabay and B. Duplantier, J. Phys. A 15 (1982) L47-L49.
- ³⁸ H. Sompolinsky, Phys. Rev. Lett. 47 (1981) 935.
- ³⁹ H. Sompolinsky, A. Zippelius, Phys. Rev. B 25 (1982) 6860.

- ⁴⁰ H. J. Sommers, W. Dupont, J. Phys. C 17 (1984) 5785.
- ⁴¹ K. Nemoto, J. Phys. C 20 (1987) 1325.
- ⁴² A. Crisanti, T. Rizzo, Phys. Rev. E 65 (2002) 046137.
- ⁴³ A. Crisanti, L. Leuzzi and G. Parisi, J. Phys. A : Math. Gen. 35 (2002) 481.
- ⁴⁴ S. A. Orszag, Studies in applied mathematics (Cambridge University, Cambridge, 1971, Vol. 4).
- ⁴⁵ J. H. Ferziger and M. Peric, Computational Methods for Fluid Dynamics (Springer-Verlag, Berlin, 1996).
- ⁴⁶ A. Montanari, M. Müller and M. Mezard, e-print cond-mat 0307040.
- ⁴⁷ M. Müller, A. Montanari and M. Mezard, e-print cond-mat 0401139.
- ⁴⁸ P. Montishaw, Europhys. Lett. 1 (1986) 409.
- ⁴⁹ D. J. Thouless, P. W. Anderson and R. G. Palmer, Phil. Mag. 35 (1977) 593.
- ⁵⁰ A. Caiazzo, A. Crisanti and L. Leuzzi, in preparation
- ⁵¹ D. J. Thouless, J. R. de Almeida and J. M. Kosterlitz, J. Phys. C 13 (1980) 3271.
- ⁵² H. J. Sommers, J. Phys. Lett. 46 (1985) L-779.
- ⁵³ I. Y. Korenblit, E. F. Shender, Sov. Phys. JETP 62, 1030 (1986).
- ⁵⁴ Indeed, the important aspect of mean field models is that this calculation can actually be carried out, whereas for short range disordered models the free energy is beyond the reach of analytical computation.
- ⁵⁵ In the dynamical approach of Sompolinsky^{38,39} to the spin glass problem represents, in the Fluctuation-Dissipation Relation (FDR), the anomaly in the linear response with respect to the equilibrium value